黎红梅,杨石岭. 2025. 白垩纪-古近纪热室气候与火事件. 岩石学报,41(10): 3562 – 3577, doi: 10.18654/1000-0569/2025.10.19; CSTR: 32089.14.APS-ysxb.2025.10.19

白垩纪-古近纪热室气候与火事件*

黎红梅[1,2] 杨石岭[1,2**]

LI HongMei[1,2] and YANG ShiLing[1,2 **]

1. 中国科学院地质与地球物理研究所,岩石圈演化与环境演变全国重点实验室, 北京 100029
2. 中国科学院大学地球与行星科学学院, 北京 100049

1. *State Key Laboratory of Lithospheric and Environmental Coevolution, Institute of Geology and Geophysics, Chinese Academy of Sciences, Beijing* 100029, *China*
2. *College of Earth and Planetary Sciences, University of Chinese Academy of Sciences, Beijing* 100049, *China*

2025-04-18 收稿, 2025-07-18 改回.

Li HM and Yang SL. 2025. Climate and fire events during the Cretaceous-Paleogene hothouse period. *Acta Petrologica Sinica*, 41(10): 3562 – 3577, doi: 10.18654/1000-0569/2025.10.19; CSTR: 32089.14.APS-ysxb.2025.10.19

Abstract Recent increases in carbon emissions have driven global temperatures upward, significantly elevating wildfire risks and posing substantial challenges to ecosystems. The Mid-Cretaceous (110 ~ 82Ma) and Early Paleogene (56 ~ 47Ma) periods represent two characteristic hothouse periods that serve as crucial geological analogs for understanding potential future extreme climates and their ecological impacts. This study examines the Cretaceous-Paleogene hothouse period by compiling fire event proxies, including black carbon records, to analyze paleofire characteristics and their relationship with hothouse environments. We conduct a comparative analysis of paleofire patterns between these two periods and investigate their underlying controlling factors. Our key findings reveal: (1) Fire events were predominantly concentrated in the mid-latitude regions of the Northern Hemisphere during both hothouse periods, with geological evidence and climate modeling suggesting that pronounced seasonal climate variations in these regions facilitated fire occurrences; (2) The Cretaceous hothouse period experienced more frequent fire events compared to the Paleogene hothouse period; (3) Elevated temperatures and atmospheric oxygen levels during the Cretaceous hothouse period created favorable conditions for fire activity, while changes in vegetation composition and reduced climatic seasonality during the Paleogene hothouse period suppressed fire occurrence. Future research should prioritize the comprehensive analysis of fire proxies, the development of deep-time paleofire databases, and the assimilation of paleoclimate data to advance understanding of the coupled interactions among fire regimes, vegetation dynamics, and hothouse climates. Such efforts will provide critical insights for projecting future wildfire trends and ecological responses under sustained global warming.

Key words Hothouse climate; Fire events; Black carbon; Vegetation; Cretaceous; Paleogene

摘 要 近年来随着碳排放的加剧,全球温度不断攀升,导致火灾风险激增,使生态系统面临很大挑战。白垩纪中期(110 ~82Ma)与古近纪早期(56 ~47Ma)是两个典型的“热室期”,为理解未来可能面临的极热气候及其生态效应提供了重要地质参照。本文聚焦白垩纪和古近纪热室期,搜集黑碳等指示的火事件记录,分析古火特征及其与热室环境的关系。在此基础上,比较了两个热室期的古火差异并探讨了其潜在影响因素。结果显示:(1)热室期火事件主要集中在北半球中纬度地区,地质记录与数值模拟表明该区域的季节性变化有利于火事件的发生;(2)白垩纪热室期火事件较多,古近纪热室期火事件相对较少;(3)白垩纪热室期的高温、高大气 O_2 浓度为火活动提供了有利条件,而古近纪热室期的植被组成和气候季节性的不明显,抑制了火活动。未来研究应注重火指标的综合分析,构建深时火数据库,结合古气候数据同化技术,深入探究火-植被-热室气候的耦合关系,为预测未来气候变暖下的火活动变化及其生态响应提供科学依据。

* 本文受国家重点研发计划项目(2022YFF0800800)、国家自然科学基金项目(92479208)和中国科学院地质与地球物理研究所重点部署项目(IGGCAS-201905)联合资助.

第一作者简介: 黎红梅,女,2001 年生,硕士生,第四纪地质专业,E-mail: lqh96785@163.com

** **通讯作者**:杨石岭,男,1974 年生,博士,研究员,从事古环境研究,E-mail: yangsl@mail.iggcas.ac.cn

关键词 热室气候；火事件；黑碳；植被；白垩纪；古近纪
中图法分类号 P532；P534

火是陆地生态系统的重要组成部分（McLauchlan *et al.*，2020），通过释放 CO_2 等温室气体，对全球碳循环和气候系统产生了深刻影响（Page *et al.*，2002；Bowman *et al.*，2009）。随着化石燃料的消耗，全球温度不断攀升。最新数据显示，2024 年全球平均地表温度较工业化前水平（1850～1900 年基线）升高 1.55℃（Copernicus，2024；WMO，2025），全球变暖导致全球火灾频率和强度显著上升（Jones *et al.*，2020；Cunningham *et al.*，2024）。据统计，2003～2023 年，全球极端火事件发生频率增加了 2.2 倍（Cunningham *et al.*，2024），北美洲西部、南美洲多个地区火灾肆虐（Cunningham *et al.*，2024；WMO，2025），使生态系统面临严峻挑战。考虑到未来碳排放还可能进一步加剧，以当前的增温速率估算，2300 年前后地球气候或将进入“热室”状态（Scotese *et al.*，2021）。因此，探讨增温背景下火的特征及其对生态环境的影响，是我们面临的紧迫知识需求。

白垩纪-古近纪（128～39.4Ma）是距今最近的热室期（Scotese *et al.*，2021），以白垩纪中期（110～82Ma）和古近纪早期（56～47Ma）为代表（Westerhold *et al.*，2020），主要特征是“高温”（全球年平均温度大于 20℃、两极地区呈无冰状态）（Scotese *et al.*，2021；Judd *et al.*，2024）、“高 CO_2 浓度”（600×10^{-6}以上）（The Cenozoic CO_2 Proxy Integration Project，CenCO$_2$PIP）（Consortium，2023；Judd *et al.*，2024）（图 1a，b）。在此期间，地球表层环境发生显著变化：全球海平面整体上升（Haq，2014；Miller *et al.*，2020）（图 1c，d）；热带、亚热带向高纬极地扩张，高低纬气候梯度变化不明显（van Dijk *et al.*，2020；Gaskell *et al.*，2022）；被子植物出现，逐渐代替裸子植物占据主导地位（Heimhofer *et al.*，2005；Friis *et al.*，2006）（图 1e）。已有研究表明，两个热室期的形成与地球深部过程碳的剧烈释放密切相关（Jiang and Lee，2019；陈祚伶，2022；张少华等，2022），是探究气候环境和火活动特征机理的理想时段。

黑碳（Black Carbon，BC）是生物质和化石燃料不完全燃烧产生的一系列含碳物质（黑碳连续体）（Goldberg，1985；Hedges *et al.*，2000），具有高度浓缩的芳香结构（Smith and Chughtai，1995），性质稳定，可以长期保存于土壤与沉积物之中（Kuhlbusch，1998）。自 Smith *et al.*（1973）首次发现海洋沉积的黑碳记录以来，黑碳已成为重建古火历史的重要指标（Suman *et al.*，1997；Scott，2000）。Moore and Kurtz（2008）利用美国新泽西州边缘海与远洋沉积物中的黑碳，对古新世-始新世极热事件（Paleocene-Eocene Thermal Maximum，PETM；～56Ma）触发机制的“野火假说”提出了质疑；Baker *et al.*（2020）和 Xu *et al.*（2022）基于黑碳等记录发现火活动加剧了陆地风化，促进营养物质输入海洋，与大洋缺氧事件（Oceanic Anoxic Events，OAEs）存在紧密关联；众多炭化植物的发现也为白垩纪热室期被子植物的快速演化提供了重要支撑（Bond and Scott，2010；Brown *et al.*，2012）。对此，本文梳理并分析了白垩纪和古近纪热室期的黑碳记录，以这些记录反映的火事件为切入点，重点探讨了黑碳等指标的古火指示意义以及古火与热室环境的联系。另外，本文还比较了两个热室期的火差异及其潜在影响因素，为理解未来高温背景下火灾风险和植被响应提供地质参考。

1 热室环境特征

1.1 白垩纪热室期

白垩纪热室期的典型高温阶段以土伦期（～92Ma）为代表（Huber *et al.*，2018），平均温度达到了 36℃（Judd *et al.*，2024）。高纬地区对热室期气候的响应较为明显，南极地区出现以针叶树为主的温带雨林（Klages *et al.*，2020），北美阿拉斯加地区生长着蕨类、裸子植物针叶树（Fiorillo *et al.*，2012）。

白垩纪热室期与地球深部活动关系密切（胡修棉等，2020）。地球深部活动频繁，巨量的碳被携带到表层系统，导致大气中 CO_2、CH_4 等大幅增加，进而引发了全球变暖和大洋缺氧事件（Schlanger and Jenkyns，1976）。期间，一些营养元素随着岩石风化、侵蚀、搬运等过程流入海洋（Kraal *et al.*，2010），增强了表层海洋生产力和以黑色页岩为代表的有机碳埋藏，促进了大气中 O_2 分压增加。

1.2 古近纪热室期

古近纪热室期以古新世-始新世极热事件和早始新世（53～49Ma）为代表（Inglis *et al.*，2020；Westerhold *et al.*，2020）。PETM 期间，巨量轻碳涌入大气，引起全球短时间内急剧增温超过 5℃（Tierney *et al.*，2022），海水酸化（Penman *et al.*，2014；Li *et al.*，2024）、深层缺氧（Dickson *et al.*，2014），底栖有孔虫灭绝 30%～50%（Thomas，2007）。海洋环流模式被异常升温扰乱，底层水集中区由南半球转移到北半球（Nunes and Norris，2006）。同时，气候变暖驱动了高纬地区生长连续的森林带，为树栖灵长目 *Teilhardina* 属提供了生态廊道，促使其跨大陆迁移（Smith *et al.*，2006）。

早始新世期间，全球普遍变暖，高纬地区显著升温，高低纬之间的温度梯度减小（Huber and Caballero，2011；Eichenseer and Jones，2024）。全球水循环增强，中高纬地区降水量显著增加（Huber and Caballero，2003）。孢粉与生标记录表明，南极威尔克斯地的边缘地区生长着棕榈科（Arecaceae）、桫椤科（Cyatheaceae）等低纬气候区的植物（Pross *et al.*，2012），北极地区的植被也从针叶林向阔叶林转变（Willard *et al.*，2019）。

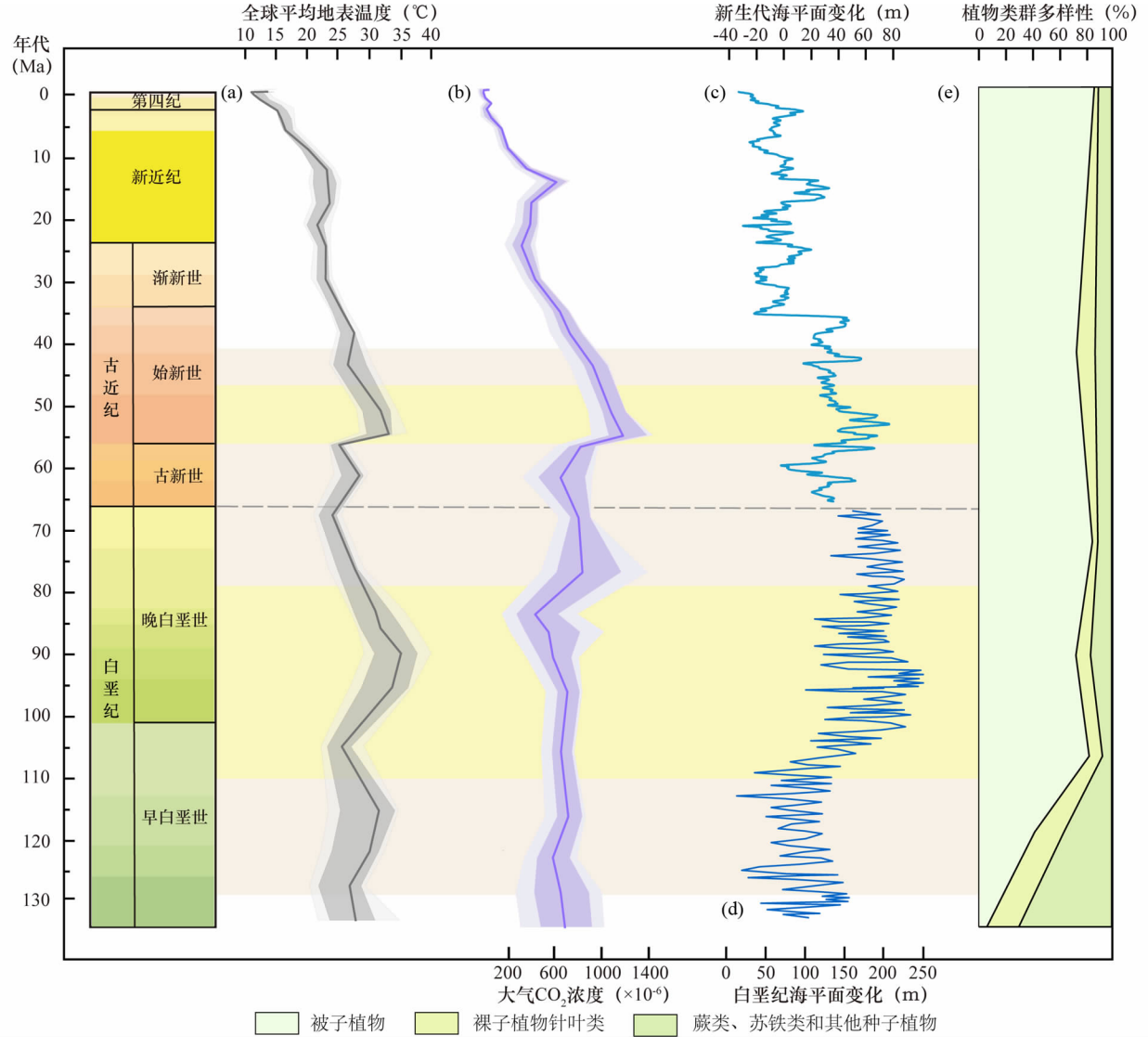


图 1 白垩纪以来的气候环境记录

(a)全球平均地表温度(浅灰色和深灰色区域分别代表 90%、68% 的置信区间)(Judd *et al.*, 2024);(b)大气 CO_2 浓度(浅紫色和深紫色区域分别代表 90%、68% 的置信区间)(Judd *et al.*, 2024);(c)新生代海平面变化(Miller *et al.*, 2020);(d)白垩纪海平面变化(Haq, 2014);(e)植物类群多样性(Lidgard and Crane, 1988; de Boer *et al.*, 2012). 水平阴影区指示白垩纪-古近纪热室期

Fig. 1 Climatic and environmental records since the Cretaceous

(a) global mean surface temperature (light grey and dark grey areas represent 90% and 68% confidence intervals, respectively) (Judd *et al.*, 2024); (b) atmospheric CO_2 concentration (light purple and dark purple areas represent 90% and 68% confidence intervals, respectively) (Judd *et al.*, 2024); (c) global mean sea level during the Cenozoic (Miller *et al.*, 2020); (d) sea level fluctuations during the Cretaceous (Haq, 2014); (e) diversity of Plant Groups (Lidgard and Crane, 1988; de Boer *et al.*, 2012). The horizontal shaded area indicates the Cretaceous-Paleogene hothouse period

2 指标与方法

2.1 火与火指标

火作为地表系统的重要驱动力,与气候、植被、生物、地球化学等过程密切相关(Harrison *et al.*, 2010),在维持生态系统的结构与功能方面起着重要作用(Bowman *et al.*, 2009; McLauchlan *et al.*, 2020)。现代火在不同生态系统的规模和频率差异显著,南美洲亚马孙雨林的火灾持续时间长(数周),非洲热带稀树草原的火灾传播速度快但持续时间短(<1 天)(Andela *et al.*, 2019)。现代天然火主要分布在北美和俄罗斯的北方林区(van der Werf *et al.*, 2017),可能与全球变暖在高纬地区最为显著及其驱动的针叶林地区逐渐干燥有关(Cunningham *et al.*, 2024)。气候是火的主要控制

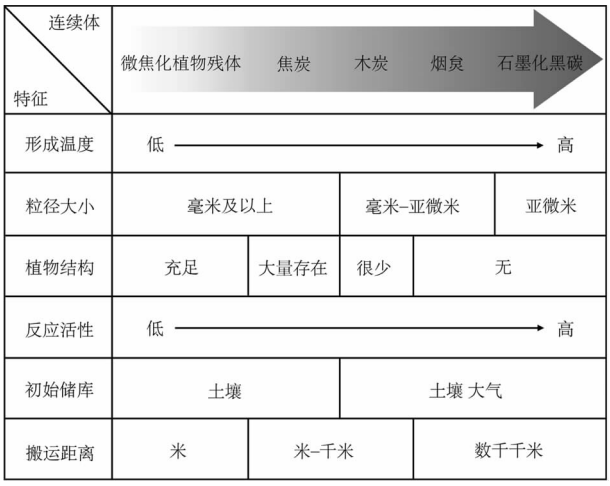


图 2 黑碳连续体及其理化性质(据 Masiello, 2004 修改)

Fig. 2 Black carbon combustion continuum and its physicochemical properties(modified after Masiello, 2004)

因素(Harrison *et al.*, 2010),气候变暖驱动着更长的火季(fire season)(Jones *et al.*, 2020; Gajendiran *et al.*, 2024),提高了火灾发生频率;另一方面,火也可以通过破坏植被及释放气体、气溶胶影响全球气候。研究显示,全球每年约有 5.9% 的植被经历过燃烧(Chen *et al.*, 2023),全球每年火灾导致的碳排放为 2.2pg(van der Werf *et al.*, 2017)。适度的火扰动能够促进植被结构演化,比如火灾导致的树皮增厚、耐火性增强(He *et al.*, 2012),但极端火灾往往导致植被结构剧变,使生物多样性面临严重威胁(Gajendiran *et al.*, 2024)。

当前变暖背景下极端火灾频发(Cunningham *et al.*, 2024),但现代观测资料时间跨度难以揭示火-气候-植被系统的长期演化规律,探究古火事件对于理解火的长期变化机制、预测未来火活动具有重要意义。地质时期发生的火事件称为古火(paleofire)(Scott, 1989, 2000),Scott(2000)认为古火的"火三角"可以理解为大气、植被和气候,某一要素的变化将影响火灾发生的可能性、燃烧程度与燃烧产物。

沉积记录保存了长时间尺度的古火信息,本文的古火指标主要包括黑碳、煤中惰质组(inertinite)和多环芳烃(Polycyclic Aromatic Hydrocarbons,PAHs)。黑碳这一名词的提出晚于木炭(charcoal)和炭屑(microscopic charcoal,微观木炭)。自 1941 年 Iversen 观察花粉时首次发现炭屑以来,它的形态分析(Belcher and Hudspith, 2016)、传输(Clark, 1988)、沉积埋藏(Scott, 2010)、研究方法(李宜垠等, 2010)等进展颇丰。1985 年,Goldberg 首次提出"black carbon"并认为其是以碳元素为主,包含少量氢、氧、氮、硫元素的物质(Goldberg, 1985)。1999 年,Hedges 在 Goldschmidt 大会上提出黑碳连续谱模型(Hedges *et al.*, 2000),即"连续体",包括焦化植物残体(charred biomass)、焦炭(char)、木炭(charcoal)、挥发性组分重新聚合而成的烟炱(soot)及高度浓缩的石墨碳(graphitic carbon)。之后,Masiello(2004)补充了连续体的理化性质(图 2)。煤中惰质组(煤岩学领域木炭的代名词)(Glasspool and Scott, 2010)最主要的成因与燃烧过程有关(Scott, 2010);惰质组中的丝质体和半丝质体一般保存植物结构并具有相对较高的反射率(ICCP, 2001),近年来被广泛用于古火和大气 O_2 浓度重建(Glasspool and Scott, 2010; 邵龙义等, 2024)。PAHs 是由两个或多个苯环组成的芳香烃类化合物,多存在于烟炱中(Lima *et al.*, 2005)。成因一般分为两种,一种是成岩或生物过程中的有机质降解(Grice *et al.*, 2007);另一种是不完全燃烧、热解产生的 PAHs(Pyrogenic PAHs, PyroPAHs),多为高分子量 PAHs(4 环及以上)(Lima *et al.*, 2005)。各项火指标及其指示意义详见表 1。

2.2 分析方法

本文搜集了白垩纪和古近纪热室期的火记录(表 2、表 3),通过黑碳或多环芳烃、煤中惰质组和木炭三种指标识别古火,分析白垩纪阿尔布期、塞诺曼期、土伦期、康尼亚克期、圣通期及古近纪 PETM、早始新世的古火频次。为避免重复统计,同一地点、同一时间段的火事件只统计一次。通过 GPlates 2.3.0 软件(https://www.earthbyte.org/category/gplates/)重建火记录在白垩纪、古近纪热室期的经纬度,获得白垩纪热室期 111 个点位和古近纪热室期 15 个点位的火事件。参考 Scotese(2016)的古地理图,将火事件点位绘制其中(图 3)。

3 结果

从火事件的数量看(表 2、表 3),白垩纪热室期整体多于古近纪热室期。其中,白垩纪热室期的阿尔布期火事件占据最多(图 3a),其次为塞诺曼期(图 3b),土伦期和圣通期的火事件数量相近,康尼亚克期相对偏少(图 3c);古近纪热室期早始新世的火事件较少,PETM 时期的火事件相对较多(图 3d)。

从火事件的地理分布看(图 3、图 4),两个热室期的火事件均集中分布在北半球中纬度大陆地区(30°N ~ 60°N)(图 4b),且海陆交界处火事件记录多于大陆内部。相较于北半球,南半球的火事件整体偏少且分散,分布于澳大利亚、南美洲与非洲的局部地区(图 3)。

4 热室期火事件及其影响因素

4.1 白垩纪热室期

白垩纪热室期的火记录主要集中分布于北半球中纬度地区,南半球偏少且分散(图 4b)。有研究模拟重建了白垩纪不同阶段的降水分布(Valdes *et al.*, 2021; Scotese *et al.*, 2025),结果显示,白垩纪中期到末期,赤道地区形成了一条

表 1 火指标及其指示意义

Table 1 Fire proxies and their indicative significance

类型	指标和意义	指示源区	优势	局限	参考文献
黑碳	反射率、形态(木炭):指示燃烧温度、火的类型 通量/浓度:指示火的强度、频率 $\delta^{13}C$:指示燃烧源(植被类型) BC/TOC 比值:指示火的真实强度(校正 TOC 浓度波动)	粗粒径(木炭)反映局部火灾;细粒径(烟炱)反映区域或全球尺度火灾	连续体包含不同燃烧阶段的产物,根据不同产物判断火灾燃烧阶段;广布于大气、水体、土壤、沉积物、冰川等环境介质,便于跨介质对比	不同提取方法(化学氧化法、分子标志物法等)的结果存在一定差异	Masiello, 2004; Bird and Cali, 1998; Moore and Kurtz, 2008; Pang *et al.*, 2021; 祝孟博等, 2017; 王学婷等, 2025
多环芳烃	不同环数比值、PyroPAHs 浓度:指示燃烧温度、火的频率	低分子量与高分子量 PAHs 比值:高比值(0.75~0.95)反映远距离搬运;低比值(0.35~0.8)反映原地沉积	样品用量少;可为黑碳稀少的地区(如极地)提供火灾证据,扩展古火重建的空间范围	燃烧并非 PAHs 的唯一来源,需要区分石油等成因	Karp *et al.*, 2020; Denis *et al.*, 2017; Boudinot and Sepúlveda, 2020
煤中惰质组	反射率、形态:指示燃烧温度、火的类型	原地或近源	结构稳定,利用其在煤中的相对丰度可以重建大气氧气浓度	局限于煤(泥炭)沉积环境,记录的时空范围相对有限	Jones *et al.*, 1991, 1993; ICCP, 2001; Glasspool and Scott, 2010

表 2 白垩纪热室期火事件

Table 2 Fire events during the Cretaceous hothouse period

序号	热室期	火指标	地点	古纬度(°)	古经度(°)	参考文献
1	阿尔布期	PAHs	日本中部富山县	49.0	134.2	Hasegawa and Hibino, 2011; Lü *et al.*, 2024
2	阿尔布期	惰质组,PAHs	中国松辽盆地	51.4	120.4	Zhang *et al.*, 2022
3	阿尔布期	惰质组,PAHs	中国阜新盆地	45.3	117.9	Xu *et al.*, 2022
4	阿尔布期	惰质组,PAHs	中国海拉尔盆地	52.4	113.6	Wang *et al.*, 2023
5	阿尔布期	惰质组,PAHs	尼日利亚卡拉巴尔	-4.4	-3.2	Ekot *et al.*, 2014
6	阿尔布期	惰质组	中国伊敏煤田	53.0	113.2	Moore *et al.*, 2021; Wang *et al.*, 2023
7	阿尔布期	惰质组	中国二连盆地	36.4	105.6	Wang *et al.*, 2019
8	阿尔布期	惰质组	中国三江盆地	35.5	120.2	
9	阿尔布期	惰质组	加拿大不列颠哥伦比亚省	57.8	-68.8	Lamberson *et al.*, 1996; Lü *et al.*, 2024
10	阿尔布期	惰质组	加拿大不列颠哥伦比亚省	58.3	-67.0	Chalmers and Bustin, 2007; Lü *et al.*, 2024
11	阿尔布期	惰质组	加拿大	53.2	-62.7	
12	阿尔布期	惰质组	加拿大	29.9	3.2	
13	阿尔布期	惰质组	澳大利亚昆士兰州	-59.7	143.7	Glasspool and Scott, 2010; Brown *et al.*, 2012; Lü *et al.*, 2024
14	阿尔布期	惰质组	加拿大阿尔伯塔省	46.2	-75.9	
15	阿尔布期	惰质组	加拿大不列颠哥伦比亚省	59.6	-69.3	
16	阿尔布期	惰质组	美国新泽西州	33.5	-32.6	
17	阿尔布期	木炭	美国弗吉尼亚州	31.7	-35.7	Brown *et al.*, 2012; Lü *et al.*, 2024
18	阿尔布期	木炭	美国弗吉尼亚州	35.4	-37.7	Crane and Herendeen, 1996; Brown *et al.*, 2012
19	阿尔布期	木炭	美国堪萨斯州	37.35	-54.45	Wang, 2004; Brown *et al.*, 2012; Lü *et al.*, 2024
20	阿尔布期	木炭	美国阿拉斯加州	78.73	-99.03	
21	阿尔布期	木炭	美国明尼苏达州	42.3	-47.6	Brown *et al.*, 2012; Lü *et al.*, 2024
22	阿尔布期	木炭	西班牙坎塔布里亚自治区	32.6	4.8	
23	阿尔布期	木炭	西班牙阿拉贡自治区	29.6	6.7	Vajda *et al.*, 2016; Lü *et al.*, 2024

续表 2

Continued Table 2

序号	热室期	火指标	地点	古纬度(°)	古经度(°)	参考文献
24	阿尔布期	木炭	英国英格兰东部	41.3	6.8	Herendeen and Skog, 1998
25	阿尔布期	木炭	德国北莱茵-威斯特法伦州	40.9	14.2	Uhl *et al.*, 2019; Lü *et al.*, 2024
26	阿尔布期	木炭	比利时蒙斯盆地	39.7	10.7	Yans *et al.*, 2009; Lü *et al.*, 2024
27	阿尔布期	木炭	葡萄牙中部地区	29.12	-1.22	Brown *et al.*, 2012; Friis *et al.*, 2019
28	阿尔布期	木炭	葡萄牙中部地区	31.3	-0.4	
29	阿尔布期	木炭	约旦杰拉什地区	7.3	30.8	Abu Hamad *et al.*, 2016; Lü *et al.*, 2024
30	阿尔布期	木炭	印度雷瓦盆地	-44.9	55.5	Kumar, 2018
31	阿尔布期	木炭	印度卡奇盆地	-36.8	39.9	
32	阿尔布期	木炭	凯尔盖朗高原	-47.6	62.4	Francis and Coffin, 1992
33	阿尔布期	木炭	澳大利亚昆士兰州	-60.6	126.8	Pole and Douglas, 1999; Brown *et al.*, 2012
34	阿尔布期	木炭	澳大利亚奥特威盆地	-72.4	120.2	Tosolini *et al.*, 2018; Lü *et al.*, 2024
35	阿尔布期	木炭	巴西阿拉里佩盆地	-17.1	-11.3	Martill *et al.*, 2012
36	阿尔布期	木炭	巴西阿拉里佩盆地	-10.7	-9.5	de Lima *et al.*, 2019
37	阿尔布期	木炭	巴西罗赖马州	-0.7	-30.9	dos Santos *et al.*, 2016
38	阿尔布期	木炭	阿根廷圣克鲁斯省	-53.0	-42.6	Brown *et al.*, 2012; Lü *et al.*, 2024
39	塞诺曼期	PAHs	美国西部	37.8	-72.9	Boudinot and Sepúlveda, 2020
40	塞诺曼期	PAHs	日本北海道地区	53.6	138.3	Nakamura *et al.*, 2010
41	塞诺曼期	PAHs,木炭	日本北海道地区	53.2	137.2	
42	塞诺曼期	PAHs,木炭	日本北海道地区	54.2	136.8	Hasegawa, 2001; Lü *et al.*, 2024
43	塞诺曼期	PAHs,木炭	俄罗斯萨哈林岛	57.5	136.2	
44	塞诺曼期	惰质组	美国犹他州	41.1	-71.9	Glasspool and Scott, 2010; Brown *et al.*, 2012
45	塞诺曼期	惰质组	尼日利亚卡拉巴尔	-6.9	-3.1	Ekpo *et al.*, 2012; Lü *et al.*, 2024
46	塞诺曼期	惰质组	哥伦比亚科迪勒拉地区	-3.2	-47.9	Guatame and Rincón, 2021
47	塞诺曼期	惰质组	加拿大不列颠哥伦比亚省	56.6	-73.2	Glasspool and Scott, 2010; Brown *et al.*, 2012; Lü *et al.*, 2024
48	塞诺曼期	木炭	美国堪萨斯州	36.0	-59.8	Wang, 2004; Brown *et al.*, 2012; Lü *et al.*, 2024
49	塞诺曼期	木炭	美国阿拉斯加州	59.3	-86.0	Fiorillo *et al.*, 2012
50	塞诺曼期	木炭	美国阿拉斯加州	78.0	-98.7	Brown *et al.*, 2012; Lü *et al.*, 2024
51	塞诺曼期	木炭	美国明尼苏达州	40.9	-53.1	
52	塞诺曼期	木炭	美国马里兰州	32.0	-39.2	Herendeen, 1991; Brown *et al.*, 2012
53	塞诺曼期	木炭	意大利坎帕尼亚大区	22.0	13.9	Bartiromo *et al.*, 2019
54	塞诺曼期	木炭	德国莱茵维尔夫拉特	39.9	7.7	Viehofen *et al.*, 2008
55	塞诺曼期	木炭	捷克波西米亚盆地	39.2	13.9	Kvaček and Eklund, 2003; Brown *et al.*, 2012; Lü *et al.*, 2024
56	塞诺曼期	木炭	捷克波西米亚盆地	39.8	13.0	Greguš *et al.*, 2020
57	塞诺曼期	木炭	捷克东部	38.8	16.0	Falcon-Lang *et al.*, 2001; Brown *et al.*, 2012
58	塞诺曼期	木炭	埃及西部	9.7	24.8	El Atfy *et al.*, 2023
59	塞诺曼期	木炭	缅甸克钦邦	12.8	94.5	Peng *et al.*, 2022; Lü *et al.*, 2024
60	塞诺曼期	木炭	阿根廷圣克鲁斯省	-56.6	-48.4	Brown *et al.*, 2012; Lü *et al.*, 2024
61	塞诺曼期	木炭	澳大利亚昆士兰州	-56.9	131.3	
62	塞诺曼期	木炭	新西兰查塔姆群岛	-80.4	-138.2	Mays and Cantrill, 2019
63	土伦期	PAHs	加拿大斯韦尔德普盆地	72.2	-14.6	Synnott *et al.*, 2021
64	土伦期	PAHs	美国西部	41.3	-77.6	Boudinot and Sepúlveda, 2020
65	土伦期	PAHs	日本北海道地区	50.9	135.4	Nakamura *et al.*, 2010
66	土伦期	PAHs,木炭	日本北海道地区	50.5	134.4	
67	土伦期	PAHs,木炭	日本北海道地区	51.6	134.1	Hasegawa, 2001; Lü *et al.*, 2024
68	土伦期	PAHs,木炭	俄罗斯萨哈林岛	54.8	133.5	
69	土伦期	惰质组	尼日利亚卡拉巴尔	-5.0	-2.4	Ekpo *et al.*, 2012; Lü *et al.*, 2024
70	土伦期	惰质组	美国犹他州	33.9	-51.6	Glasspool and Scott, 2010; Brown *et al.*, 2012; Lü *et al.*, 2024
71	土伦期	惰质组	美国犹他州	44.5	-76.7	
72	土伦期	惰质组	美国新墨西哥州	39.8	-74.6	

续表 2

Continued Table 2

序号	热室期	火指标	地点	古纬度(°)	古经度(°)	参考文献
73	土伦期	惰质组	加拿大温哥华岛	51.2	-89.7	
74	土伦期	惰质组	加拿大不列颠哥伦比亚省	60.0	-78.6	
75	土伦期	惰质组	尼日利亚贝努埃裂谷盆地	-6.7	0.9	Akinyemi *et al.*, 2022
76	土伦期	惰质组	哥伦比亚科迪勒拉地区	-1.5	-50.4	Guatame and Rincón, 2021
77	土伦期	木炭	美国新墨西哥州	36.9	-76.5	Sweeney *et al.*, 2009; Lü *et al.*, 2024
78	土伦期	木炭	美国阿拉斯加州	63.4	-92.9	Fiorillo *et al.*, 2012
79	土伦期	木炭	新西兰查塔姆群岛	-75.1	-130.7	Mays *et al.*, 2017
80	土伦期	木炭	澳大利亚邦迪盆地	-50.7	124.8	Carpenter *et al.*, 2016
81	康尼亚克期	PAHs	加拿大斯韦尔德普盆地	72.2	-14.6	Synnott *et al.*, 2021
82	康尼亚克期	PAHs	日本本州岛北部	50.03	132.49	Nakamura *et al.*, 2010
83	康尼亚克期	PAHs,木炭	南极利文斯顿岛	-66.1	-59.2	Kostova *et al.*, 2022; Lü *et al.*, 2024
84	康尼亚克期	PAHs,木炭	俄罗斯萨哈林岛	54.77	133.46	Hasegawa, 2001; Lü *et al.*, 2024
85	康尼亚克期	惰质组	尼日利亚卡拉巴尔	-5.1	-1.7	Ekpo *et al.*, 2012; Lü *et al.*, 2024
86	康尼亚克期	惰质组	哥伦比亚科迪勒拉地区	-1.5	-50.4	Guatame and Rincón, 2021
87	康尼亚克期	惰质组	美国犹他州	33.9	-51.6	
88	康尼亚克期	惰质组	美国犹他州	41.3	-77.6	Glasspool and Scott, 2010; Brown *et al.*, 2012; Lü *et al.*, 2024
89	康尼亚克期	惰质组	美国新墨西哥州	39.8	-74.6	
90	康尼亚克期	惰质组	加拿大温哥华岛	51.2	-89.7	
91	康尼亚克期	惰质组	尼日利亚贝努厄裂谷盆地	-6.7	0.9	Akinyemi *et al.*, 2022
92	康尼亚克期	木炭	葡萄牙阿威罗地区	30.8	-5.7	Herendeen, 1991; Brown *et al.*, 2012
93	康尼亚克期	木炭	澳大利亚邦迪盆地	-50.7	124.8	Carpenter *et al.*, 2016
94	圣通期	黑碳,PAHs	中国松辽盆地	40.9	113.1	祝孟博等, 2017; Lei *et al.*, 2022
95	圣通期	PAHs	加拿大斯韦尔德普盆地	73.5	-6.1	Synnott *et al.*, 2021
96	圣通期	PAHs,木炭	南极利文斯顿岛	-60.3	-70.5	Kostova *et al.*, 2022; Lü *et al.*, 2024
97	圣通期	PAHs,木炭	俄罗斯萨哈林岛	52.3	130.3	Hasegawa, 2001; Lü *et al.*, 2024
98	圣通期	惰质组	美国犹他州	45.1	-80.5	Glasspool and Scott, 2010; Brown *et al.*, 2012; Lü *et al.*, 2024
99	圣通期	惰质组	美国新墨西哥州	43.6	-77.3	
100	圣通期	惰质组	加拿大温哥华岛	56.0	-92.8	
101	圣通期	惰质组	哥伦比亚科迪勒拉地区	1.4	-52.0	Guatame and Rincón, 2021
102	圣通期	惰质组	尼日利亚贝努厄裂谷盆地	-3.7	5.9	Akinyemi *et al.*, 2022
103	圣通期	木炭	美国乔治亚州	34.2	-55.0	Falcon-Lang *et al.*, 2012; Lü *et al.*, 2024
104	圣通期	木炭	美国乔治亚州	34.0	-54.2	Brown *et al.*, 2012
105	圣通期	木炭	美国怀俄明州	49.5	-73.8	Glasspool and Scott, 2010; Brown *et al.*, 2012; Lü *et al.*, 2024
106	圣通期	木炭	美国亚利桑那州	42.1	-81.8	Finkelstein *et al.*, 2005; Brown *et al.*, 2012
107	圣通期	木炭	美国阿拉巴马州	33.9	-55.3	Knight *et al.*, 2010; Lü *et al.*, 2024
108	圣通期	木炭	葡萄牙阿威罗地区	31.2	-4.9	Herendeen, 1991; Brown *et al.*, 2012
109	圣通期	木炭	澳大利亚邦迪盆地	-49.9	131.4	Carpenter *et al.*, 2016
110	圣通期	木炭	南极地区	-69.1	-75.8	Eklund *et al.*, 2004
111	圣通期	木炭	瑞典斯科讷省阿森地区	45.9	15.1	Herendeen, 1991; Brown *et al.*, 2012

注:古经纬度中的"—"代表南纬和西经;同一地点有多项火指标,首选第一个指标进行分类;阿尔布期:113.2~100.5Ma;塞诺曼期:100.5~93.9Ma;土伦期:93.9~89.8Ma;康尼亚克期:89.8~85.7Ma;圣通期:85.7~83.6Ma(绝对地质年代参考国际年代地层表-2024 年 12 月版)

表 3 古近纪热室期火事件

Table 3 Fire events during the Paleogene hothouse period

序号	热室期	火指标	地点	古纬度(°)	古经度(°)	参考文献
1	PETM	黑碳	中国南阳盆地	32.13	104.84	王学婷等, 2025
2	PETM	黑碳	美国东部	50.14	-57.92	Moore and Kurtz, 2008
3	PETM	黑碳,PAHs	中国抚顺盆地	43.34	116.03	王学婷等, 2025; Chen *et al.*, 2025
4	PETM	PAHs	中国江汉盆地	29.08	116.88	Chen *et al.*, 2025
5	PETM	PAHs	美国怀俄明州	49.79	-88.94	Denis, 2016; Denis *et al.*, 2017

续表 3

Continued Table 3

序号	热室期	火指标	地点	古纬度(°)	古经度(°)	参考文献
6	PETM	PAHs	北极罗蒙诺索夫海岭	82.65	24.23	Denis *et al.*, 2017
7	PETM	惰质组	英国南部煤矿	56.19	-13.01	Collinson *et al.*, 2007; Baker, 2022
8	PETM	木炭,PAHs	美国东部威尔逊湖	50.26	-58.85	Fung *et al.*, 2019; Baker, 2022
9	PETM	木炭,PAHs	美国东部	49.32	-60.95	
10	PETM	木炭	印度巴莫盆地	-2.18	67.52	Kumar *et al.*, 2023
11	早始新世	木炭	美国怀俄明州	46.96	-92.33	Hyland and Sheldon, 2013; Baker, 2022
12	早始新世	木炭	德国北部地区	47.76	7.72	Lenz *et al.*, 2021
13	早始新世	木炭	中国二连盆地	42.34	103.2	Zhou *et al.*, 2023
14	早始新世	惰质组	印度西部煤矿	-6.08	60.46	Rajak *et al.*, 2019
15	晚古新世-早始新世	木炭	印度西北部煤矿	-1.33	64.28	Shukla *et al.*, 2023

注:古经纬度中的"—"代表南纬和西经;同一地点有多项火指标,首选第一个指标进行分类;PETM:56Ma;早始新世:53~49Ma

从阿拉伯半岛东南端延伸至厄瓜多尔西部的湿润带,以高温高湿为特征。基于地质、地球化学和古生物等指标重建的古柯本气候带显示,随着大西洋的扩张该带年均降水显著增强(Burgener *et al.*, 2023)。这种环境影响下的植被往往含水量较高,在湿热环境的加持下不易被点燃(Lu *et al.*, 2021; Lü *et al.*, 2024)。图 3 显示,古火数据集中区域属于古柯本气候带中的 C 带(温带),且集中于该带的沿海区域。Scotese *et al.* (2025)认为该带具有强烈的气候季节性,因此该区域火记录较多可能与类似于海陆热力性质差异导致的季风气候的季节性干湿有关。

白垩纪热室期的火事件集中出现在阿尔布期(113.2~100.5Ma)和塞诺曼期(100.5~93.9Ma),其他时期相对较少。白垩纪中期(约 125~90Ma)经历了极端高温和干旱气候(Boucot *et al.*, 2013; Zhang *et al.*, 2018),这一时期被子植物数量激增、形态多样(Friis *et al.*, 2006; Benton *et al.*, 2022),对达尔文的进化论构成了巨大挑战,被称为"达尔文厌恶之谜"(Friedman, 2009)。由于被子植物的起源与快速演化问题受到学术界的广泛关注,并且阿尔布期的沉积物中本身保存着丰富的炭化被子植物(Crane and Herendeen, 1996; Bond and Scott, 2010; Brown *et al.*, 2012),这很可能是该时期火事件居多的原因之一(Lü *et al.*, 2024),但尚待更多的定量证据佐证。

4.2 古近纪热室期

古近纪热室期的火记录也主要分布在北半球中纬度地区(图 3d、图 4b),其中 PETM 的火记录相对偏多。PETM 是短时间内(<200ka)发生的极热事件(Zachos *et al.*, 2010),不同地区的水文响应不一致,极地、部分热带地区降水增加,一些内陆地区则变得更为干燥(Carmichael *et al.*, 2017)。已有研究表明,该时期的火活动存在时空差异(Denis *et al.*, 2017; Chen *et al.*, 2025),不同地区火活动的发生时间、持续时间及触发机制差异较大,反映了植被类型和气候的差异。例如,碳同位素负漂(carbon isotope excursion, CIE)期间,中国江汉盆地(Chen *et al.*, 2025)、美国大西洋沿岸的威尔逊湖火活动增强(Fung *et al.*, 2019),而中国南阳盆地(王学婷等, 2025)、抚顺盆地(Chen *et al.*, 2025)火的增强趋势则出现在 CIE 恢复阶段。

早始新世的持续时间至少要高出 PETM 一个数量级,火事件却偏少。该时期相对稳定的湿润环境(Walters *et al.*, 2023),可能抑制了季节性干旱区的大范围出现,从而降低了火灾频率与强度(Zhou *et al.*, 2023)。

4.3 白垩纪与古近纪热室期火事件差异

统计结果(表 2、表 3)显示,白垩纪热室期呈现"高火"状态,古近纪热室期呈现"低火"状态。两个热室期的一些环境要素差异较大,因此,有必要从"火三角"因素进一步比较两个热室期的火事件差异。

4.3.1 大气氧气浓度

深时大气中的氧气是影响燃料点燃以及火势蔓延的重要因素(Bond and Scott, 2010)。目前研究广泛认可的是,大气 O_2 浓度低于 15% 时,一般不会有火灾发生(Belcher and McElwain, 2008);超过 25% 时,即便是湿润的燃料也能被轻易点燃(Scott and Glasspool, 2006);达到 30% 及以上时,燃料湿度(干重)高达 112% 仍可燃烧(Belcher *et al.*, 2021),火活动可能在全球广布(Scott and Glasspool, 2006)。

整个白垩纪热室期,大气的平均 O_2 浓度可以达到 25% 以上,足以维持火灾发生。相比之下,新生代以来的大气 O_2 浓度有所下降,但仍然高于现代水平,也完全可以满足火灾的发生条件。对比来看,白垩纪热室期的火事件数量整体对应于高 O_2 浓度时期、古近纪热室期的火事件数量则明显对应于低 O_2 浓度时期(图 5)(Mills *et al.*, 2023),说明相对较低的大气 O_2 浓度可能限制了古近纪热室期的火活动。

氧气对火的促进作用在另外一些研究中也得到证实。OAE2(Oceanic Anoxic Event 2,又称 Bonarelli 事件;~94Ma)期间,北美地区的木炭和 PAHs 记录的火活动呈现增加趋势(Boudinot and Sepúlveda, 2020; Baker *et al.*, 2020; Baker, 2022),尤其是事件开始和持续期间的两次 CO_2 浓度下降期,

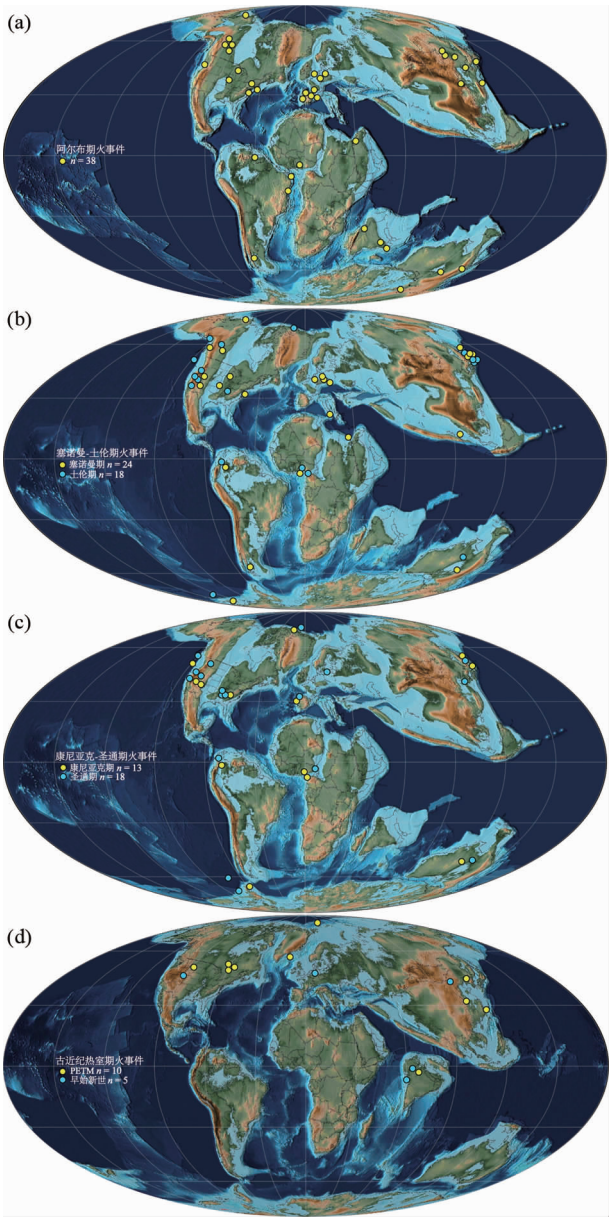


图 3 白垩纪-古近纪热室期火事件的地理分布

(a) 阿尔布期(105Ma)火事件分布图;(b)塞诺曼-土伦期(95Ma)火事件分布图;(c)康尼亚克-圣通期(绘制于时间相近的90Ma土伦期地图中)火事件分布图;(d)古近纪热室期(55Ma)火事件分布图;古地理图来自 Scotese(2016)

Fig. 3 Geographic distribution of fire events during the Cretaceous-Paleogene hothouse period

(a) distribution of fire events during the Albian (105Ma); (b) distribution of fire events during the Cenomanian-Turonian (95Ma); (c) distribution of fire events during the Coniacian-Santonian (plotted on the map of Turonian, 90Ma); (d) distribution of fire events during the Paleogene hothouse period (55Ma). Paleogeographic maps from Scotese(2016)

伴随着木炭浓度增加指示的火活动增加(Baker *et al.*, 2020)。对此,Boudinot and Sepúlveda(2020)认为火活动增加后引起营养物质输入海洋,海洋生产力提高、有机碳埋藏增加,使得大气 O_2 增加,从而再次提高了火灾频率。高频火活动后的径流、侵蚀作用加强,将磷等营养元素冲刷到海洋(Brown *et al.*, 2012)。Kraal *et al.*(2010)通过探究磷与黑色页岩及物质循环间的关系,发现 OAE2 期间大气中的 O_2 逐渐积累,最终导致了 OAE2 的终止,间接佐证了该时期的火活动与高氧状态有紧密联系。

4.3.2 燃料与植被

燃料供应是影响火灾频率的重要因素。化石证据显示,被子植物最早出现于白垩纪早期,中期扩散速度加快,晚期存在于多种生境,呈现繁盛之势(Friis *et al.*, 2006; Brodribb and Field, 2010; Brown *et al.*, 2012)。最初的被子植物主要分布在低纬地区,后来逐渐向高纬地区扩散(Lupia *et al.*, 1999; Bond and Scott, 2010)。其形态低矮,以"杂草式"(形似草本,演替迅速)生长为主(Taylor and Hickey, 1996; Brodribb and Field, 2010; Brown *et al.*, 2012),多生长在湿地、河流沿岸和火后开阔地带(Taylor and Hickey, 1996)。这种高产的"杂草式"模式具有较短的火灾周期(Bond and Scott, 2010),演替模式与现代草原火灾类似(Brown *et al.*, 2012)。火后迅速再生特征与高叶脉密度、高光合作用利用效率(Brodribb and Field, 2010)的共同作用,使其相对于裸子植物占据优势。它们在阿尔布期迅速扩散(Lupia *et al.*, 1999),后以灌木或小乔木的形式存在于裸子植物森林冠层之下(Bond and Scott, 2010; Belcher and Hudspith, 2017)。这些森林下部地表还生长着一些蕨类植物,共同组成了白垩纪热室期的植被模式,为火提供了丰富燃料。正如 Bond and Scott(2010)所述,被子植物在白垩纪的兴起,为火的发生提供新兴燃料的同时也加速了自身进化历程。

虽然早期的被子植物更替迅速,与火的耦合关系密切。但由于早期被子植物主要为草本结构,燃烧后不易保留下来成为古火证据。相比之下,具有木质特征的植物更易保存(Nichols *et al.*, 2000)。裸子植物针叶树在当时的生态系统中仍然占据一定比例(Lidgard and Crane, 1988, 1990),常见的有松科(Pinaceae)、柏科(Cupressaceae),在白垩纪热室期的古火记录中较为突出(He *et al.*, 2012)。

白垩纪末期,随着 O_2 浓度下降和火灾频率降低,闭合冠层植被扩展(Belcher *et al.*, 2021),植被封闭性增强。气候足够暖湿的情况下,火的减少会促使森林扩张(Bond *et al.*, 2005)。古近纪早期,被子植物森林开始出现(Eriksson, 2008; Belcher *et al.*, 2021)。早始新世期间,中国二连盆地的火灾频率较低,与湿润气候减少了可燃物的易燃性密切相关(Zhou *et al.*, 2023)。Denis *et al.*(2017)认为相比于裸子植物,被子植物更易促进火的传播。PETM 时期,北极地区火活动增强的主要原因在于植被类型由蕨类、裸子植物转变为被子植物。

4.3.3 热源与气候

天然火的潜在热源包括雷击、火山活动、落石撞击产生的火花、陨石撞击、自燃等,雷击最为常见(Scott, 2000)。模

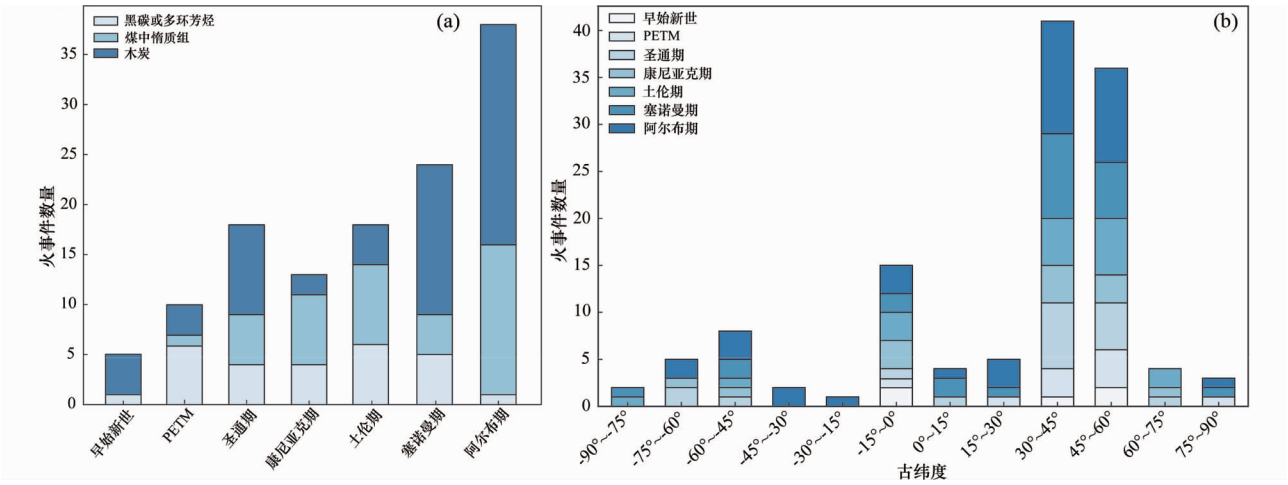


图 4　白垩纪-古近纪热室期不同时间段的火事件数量及空间分布

图 b 中古纬度“-”表示南纬

Fig. 4　The number and spatial distribution of fire events across different stages within the Cretaceous-Paleogene hothouse period

The paleolatitude in Fig. 4b: “-” represents the Southern Hemisphere

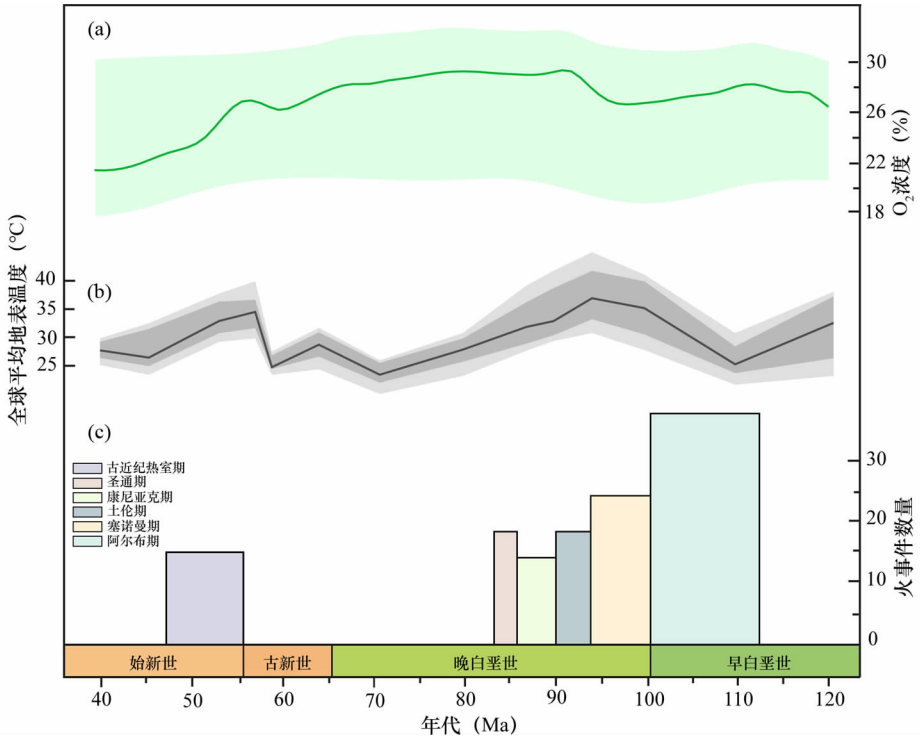


图 5　白垩纪-古近纪热室期火事件与大气 O_2 浓度、温度的对应关系

（a）大气 O_2 浓度（绿色区域代表 O_2 浓度最大值与最小值区间；Mills *et al.*，2023）；（b）全球平均地表温度（Judd *et al.*，2024）；（c）白垩纪-古近纪热室期火事件

Fig. 5　Linkages between fire events, atmospheric O_2 concentration, and temperature during the Cretaceous-Paleogene hothouse period

(a) atmospheric O_2 concentration (green area represents the range of O_2 concentrations, from the minimum to the maximum values; Mills *et al.*, 2023); (b) global mean surface temperature (Judd *et al.*, 2024); (c) fire events during the Cretaceous-Paleogene hothouse period

拟表明，高温和高 CO_2 浓度可以通过增强对流来增加闪电频率（Price and Rind, 1994），进而提高点燃燃料的可能性（Belcher *et al.*, 2010）。一些研究也发现，地质历史上的高温期火灾发生频率较高（Baker, 2022）。

如4.1所述,白垩纪热室期的"高火"状态可能受到了高温(图1、图5)和季节性干旱的驱动,至少在这种环境下更易满足火灾发生的气候条件。研究显示,火灾频率与干旱程度、植被生产力的关系呈现倒U型。火灾频率在干旱程度和植被生产力达到中等水平时最大,而在极干或极湿的环境下则较低(Bradstock, 2010; Belcher, 2013)。

古近纪热室期O_2浓度相对较低、植被封闭性增强的背景下,如果环境的季节性不显著,火灾往往难以多发或大范围蔓延。以PETM时期为例,全球变暖导致热带气旋的形成位置向极地方向移动(Kiehl *et al.*, 2021),数值模拟(Carmichael *et al.*, 2017)、陆源沉积物的高岭石等粘土矿物及其羟基同位素等(Walters *et al.*, 2022; Kumar *et al.*, 2023)佐证了暖湿范围的扩张。已搜集的古近纪热室期火事件以阴燃形式存在的占据一定比例,例如出自煤矿、泥炭环境(Collinson *et al.*, 2007; Rajak *et al.*, 2019; Shukla *et al.*, 2023)。王建等(2024)认为古新世-始新世时期的气候格局区域差异大(新特提斯与北美湿润、亚洲内陆干旱)、无显著季节变化,制约了合适的热源出现,从而导致了古近纪热室期的"低火"状态。

另外,火山活动可通过释放高温物质提供燃烧源,也能够通过植被扰动和气候调节作用影响火的发生概率(Scott, 2010, 2019)。白垩纪热室期大洋中脊快速扩张,火山活动频繁(Lee and Lackey, 2015)。火山活动不仅会释放SO_2、CO_2等气体,还会喷发熔岩流、火山碎屑流等炭化附近植被,间接引发火事件(Manfroi *et al.*, 2015, 2023)。OAE2期间多发的火山活动得到了诸多证据的支持:如海水的$^{187}Os/^{188}Os$比值突然下降(Turgeon and Creaser, 2008; Du Vivier *et al.*, 2014)、锂同位素表征的陆地风化加剧(von Strandmann *et al.*, 2013)等,为白垩纪热室期火的触发提供了可能热源。

5 结论与展望

本文基于黑碳等古火指标,分析了白垩纪和古近纪热室期的火事件情况及其反映的不同热室环境特征。结果显示,两个热室期的火事件主要集中于北半球中纬度地区。根据地质记录与数值模拟重建的气候带分布,该区域容易满足季节性干旱条件,是火事件的高发区,但尚待更多的古气候记录加以验证。

白垩纪热室期呈现"高火"状态,古近纪热室期呈现"低火"状态。白垩纪热室期的平均温度、O_2浓度要高于古近纪热室期,火活动整体上也与其有较好的对应。从火的产生和燃烧角度上看,这些是有利因素。相比之下,古近纪热室期的火活动整体偏低,虽然O_2浓度高于现代水平,但可能受到该时期的植被演化以及季节性不明显的抑制,从而制约了合适的燃料与热源出现,火难以产生或维持高频状态。

需要指出的是,不同地质时段的受关注程度、相关研究资源的可获得性、研究者的研究偏好可能会影响到我们搜集的数据数量和初步结论。但总体上看,白垩纪热室期的"高火"、古近纪热室期的"低火"与O_2浓度、植被类型及气候的关系密切。

火灾频率、强度和类型对火的解读至关重要,直接影响到对植被和气候的认识。但是,成岩作用往往会增加火指标解读的不确定性,影响火灾特征判断。运用火记录去重建火和环境变化历史,需要在准确识别沉积环境的基础上,采用多种火指标,避免依赖单一火指标,结合植物大化石、孢粉、生物标志物、沉积物中的磁学参数等综合研判。

已有研究利用火指标重建了相关时期的大气O_2浓度(Glasspool and Scott, 2010)和CO_2浓度(Schnyder *et al.*, 2009; 祝孟博, 2019),一定程度上丰富了基于火指标揭示古环境的手段。但从已有研究看,不同火指标重建的结果还存在差异。未来研究应该进一步重视火指标的解译并构建深时火数据库,加强不同地质时期的植被与气候模拟,结合古气候数据同化技术,促进我们深入理解火-植被-热室气候的耦合关系,并对预测未来提供科学支撑。

致谢 感谢纪伟强研究员在组稿中给予的大力支持;感谢周新郢研究员和张生瑞副教授两位审稿人提出的宝贵意见。

References

Abu Hamad AMB, Amireh B, Jasper A and Uhl D. 2016. New palaeobotanical data from the Jarash Formation (Aptian-Albian, Kurnub Group) of NW Jordan. Journal of Palaeosciences, 65(1-2): 19-29

Akinyemi SA, Adebayo OF, Madukwe HY, Kayode AT, Aturamu AO, OlaOlorun OA, Nyakuma BB, Jauro A, Gitari WM, Mudzielwana R and Hower JC. 2022. Elemental geochemistry and organic facies of selected cretaceous coals from the Benue Trough basin in Nigeria: Implication for paleodepositional environments. Marine and Petroleum Geology, 137: 105490

Andela N, Morton DC, Giglio L, Paugam R, Chen Y, Hantson S, van der Werf GR and Randerson JT. 2019. The global fire atlas of individual fire size, duration, speed and direction. Earth System Science Data, 11(2): 529-552

Baker SJ, Belcher CM, Barclay RS, Hesselbo SP, Laurin J and Sageman BB. 2020. CO_2-induced climate forcing on the fire record during the initiation of Cretaceous Oceanic Anoxic Event 2. GSA Bulletin, 132(1-2): 321-333

Baker SJ. 2022. Fossil evidence that increased wildfire activity occurs in tandem with periods of global warming in Earth's past. Earth-Science Reviews, 224: 103871

Bartiromo A, Graziano R, Raspini A and Bravi S. 2019. A new terrestrial plant-rich Fossil-Lagerstätte from the Middle Cenomanian (Late Cretaceous) of the Apennine Carbonate Platform (Magliano Vetere, southern Italy): Depositional and palaeoenvironmental settings. Sedimentary Geology, 388: 37-65

Belcher CM and McElwain JC. 2008. Limits for combustion in low O_2 redefine paleoatmospheric predictions for the Mesozoic. Science, 321(5893): 1197-1200

Belcher CM, Yearsley JM, Hadden RM, McElwain JC and Rein G. 2010. Baseline intrinsic flammability of Earth's ecosystems estimated from paleoatmospheric oxygen over the past 350 million years. Proceedings of the National Academy of Sciences of the United States of America, 107(52): 22448-22453

Belcher CM. 2013. Fire Phenomena and the Earth System: An Interdisciplinary Guide to Fire Science. Hoboken: Wiley-Blackwell, 97 – 112

Belcher CM and Hudspith VA. 2016. The formation of charcoal reflectance and its potential use in post-fire assessments. International Journal of Wildland Fire, 25(7): 775 – 779

Belcher CM and Hudspith VA. 2017. Changes to Cretaceous surface fire behaviour influenced the spread of the early angiosperms. New Phytologist, 213(3): 1521 – 1532

Belcher CM, Mills BJW, Vitali R, Baker SJ, Lenton TM and Watson AJ. 2021. The rise of angiosperms strengthened fire feedbacks and improved the regulation of atmospheric oxygen. Nature Communications, 12(1): 503

Benton MJ, Wilf P and Sauquet H. 2022. The angiosperm terrestrial revolution and the origins of modern biodiversity. New Phytologist, 233(5): 2017 – 2035

Bird MI and Cali JA. 1998. A million-year record of fire in sub-Saharan Africa. Nature, 394(6695): 767 – 769

Bond WJ, Woodward FI and Midgley GF. 2005. The global distribution of ecosystems in a world without fire. New Phytologist, 165(2): 525 – 538

Bond WJ and Scott AC. 2010. Fire and the spread of flowering plants in the Cretaceous. New Phytologist, 188(4): 1137 – 1150

Boucot AJ, Chen X, Scotese CR and Morley RJ. 2013. Phanerozoic Paleoclimate: An Atlas of Lithologic Indicators of Climate. Tulsa, Oklahoma, USA: Society for Sedimentary Geology

Boudinot FG and Sepúlveda J. 2020. Marine organic carbon burial increased forest fire frequency during Oceanic Anoxic Event 2. Nature Geoscience, 13(10): 693 – 698

Bowman DMJS, Balch JK, Artaxo P, Bond WJ, Carlson JM, Cochrane MA, D'Antonio CM, DeFries RS, Doyle JC, Harrison SP, Johnston FH, Keeley JE, Krawchuk MA, Kull CA, Marston JB, Moritz MA, Prentice IC, Roos CI, Scott AC, Swetnam TW, van Der Werf GR and Pyne SJ. 2009. Fire in the earth system. Science, 324(5926): 481 – 484

Bradstock RA. 2010. A biogeographic model of fire regimes in Australia: Current and future implications. Global Ecology and Biogeography, 19(2): 145 – 158

Brodribb TJ and Feild TS. 2010. Leaf hydraulic evolution led a surge in leaf photosynthetic capacity during early angiosperm diversification. Ecology Letters, 13(2): 175 – 183

Brown SAE, Scott AC, Glasspool IJ and Collinson ME. 2012. Cretaceous wildfires and their impact on the Earth System. Cretaceous Research, 36: 162 – 190

Burgener L, Hyland E, Reich BJ and Scotese C. 2023. Cretaceous climates: Mapping paleo-Köppen climatic zones using a Bayesian statistical analysis of lithologic, paleontologic, and geochemical proxies. Palaeogeography, Palaeoclimatology, Palaeoecology, 613: 111373

Carmichael MJ, Inglis GN, Badger MPS, Naafs BDA, Behrooz L, Remmelzwaal S, Monteiro FM, Rohrssen M, Farnsworth A, Buss HL, Dickson AJ, Valdes PJ, Lunt DJ and Pancost RD. 2017. Hydrological and associated biogeochemical consequences of rapid global warming during the Paleocene-Eocene Thermal Maximum. Global and Planetary Change, 157: 114 – 138

Carpenter RJ, Holman AI, Abell AD and Grice K. 2016. Cretaceous fire in Australia: A review with new geochemical evidence, and relevance to the rise of the angiosperms. Australian Journal of Botany, 64(8): 564 – 578

Chalmers GRL and Bustin RM. 2007. The organic matter distribution and methane capacity of the Lower Cretaceous strata of Northeastern British Columbia, Canada. International Journal of Coal Geology, 70 (1 – 3): 223 – 239

Chen Y, Hall J, van Wees D, Andela N, Hantson S, Giglio L, van der Werf GR, Morton DC and Randerson JT. 2023. Multi-decadal trends and variability in burned area from the fifth version of the Global Fire Emissions Database (GFED5). Earth System Science Data, 15(11): 5227 – 5259

Chen ZL. 2022. Carbon-cycle dynamics during the Paleocene-Eocene Thermal Maximum. Chinese Science Bulletin, 67(15): 1704 – 1714 (in Chinese with English abstract)

Chen ZL, Li CY, Yang SL, Lü PZ, Tang ZH, Sun JM, Ni XJ, Fang HL and Ding ZL. 2025. Two sites in East Asia add to spatiotemporal heterogeneity of wildfire activity across the Paleocene-Eocene Thermal Maximum. Geophysical Research Letters, 52 (2): e2024GL113829

Clark JS. 1988. Particle motion and the theory of charcoal analysis: Source area, transport, deposition, and sampling. Quaternary Research, 30(1): 67 – 80

Collinson ME, Steart DC, Scott AC, Glasspool IJ and Hooker JJ. 2007. Episodic fire, runoff and deposition at the Palaeocene-Eocene boundary. Journal of the Geological Society, 164(1): 87 – 97

Copernicus. 2024. Copernicus: June 2024 marks 12th month of global temperature reaching 1.5℃ above pre-industrial. https://climate.copernicus.eu/copernicus-june-2024-marks-12th-month-global-temperature-reaching-15degc-above-pre-industrial

Crane PR and Herendeen PS. 1996. Cretaceous floras containing angiosperm flowers and fruits from eastern North America. Review of Palaeobotany and Palynology, 90(3 – 4): 319 – 337

Cunningham CX, Williamson GJ and Bowman DMJS. 2024. Increasing frequency and intensity of the most extreme wildfires on Earth. Nature Ecology & Evolution, 8(8): 1420 – 1425

de Boer HJ, Eppinga MB, Wassen MJ and Dekker SC. 2012. A critical transition in leaf evolution facilitated the Cretaceous angiosperm revolution. Nature Communications, 3(1): 1221

de Lima FJ, Pires EF, Jasper A, Uhl D, Saraiva AáF and Sayão JM. 2019. Fire in the paradise: Evidence of repeated palaeo-wildfires from the Araripe Fossil Lagerstätte (Araripe Basin, Aptian-Albian), Northeast Brazil. Palaeobiodiversity and Palaeoenvironments, 99 (3): 367 – 378

Denis EH. 2016. Production and preservation of organic and fire-derived carbon across the Paleocene-Eocene Thermal Maximum. Ph. D. Dissertation. State College: The Pennsylvania State University, 89 – 109

Denis EH, Pedentchouk N, Schouten S, Pagani M and Freeman KH. 2017. Fire and ecosystem change in the Arctic across the Paleocene-Eocene Thermal Maximum. Earth and Planetary Science Letters, 467: 149 – 156

Dickson AJ, Rees-Owen RL, März C, Coe AL, Cohen AS, Pancost RD, Taylor K and Shcherbinina E. 2014. The spread of marine anoxia on the northern Tethys margin during the Paleocene-Eocene Thermal Maximum. Paleoceanography, 29(6): 471 – 488

dos Santos ÂCS, Holanda EC, de Souza V, Guerra-Sommer M, Manfroi J, Uhl D and Jasper A. 2016. Evidence of palaeo-wildfire from the upper Lower Cretaceous (Serra do Tucano Formation, Aptian-Albian) of Roraima (North Brazil). Cretaceous Research, 57: 46 – 49

Du Vivier ADC, Selby D, Sageman BB, Jarvis I, Gröcke DR and Voigt S. 2014. Marine $^{187}Os/^{188}Os$ isotope stratigraphy reveals the interaction of volcanism and ocean circulation during Oceanic Anoxic Event 2. Earth and Planetary Science Letters, 389: 23 – 33

El Atfy H, Coiffard C, El Beialy SY and Uhl D. 2023. Vegetation and climate change at the southern margin of the Neo-Tethys during the Cenomanian (Late Cretaceous): Evidence from Egypt. PLoS One, 18(1): e0281008

Eichenseer K and Jones LA. 2024. Bayesian multi-proxy reconstruction of Early Eocene latitudinal temperature gradients. Climate of the Past, 20(2): 349 – 362

Eklund H, Cantrill DJ and Francis JE. 2004. Late Cretaceous plant mesofossils from Table Nunatak, Antarctica. Cretaceous Research, 25(2): 211 – 228

Ekot AE, Igwuagwu CJ, Onyekuru SO and Bassey CE. 2014. Geochemical evaluation of thermal maturity of the Cretaceous sediments in the Calabar Flank based on the distribution of the polynuclear aromatic hydrocarbons. IOSR Journal of Applied Geology and Geophysics, 2(6): 1 – 7

Ekpo BO, Ibok UJ, Essien N and Wehner H. 2012. Geochemistry and organic petrography of Cretaceous sediments of the Calabar Flank, southeastern, Nigeria. Marine and Petroleum Geology, 35(1): 252 – 268

Eriksson O. 2008. Evolution of seed size and biotic seed dispersal in angiosperms: Paleoecological and Neoecological evidence. International Journal of Plant Sciences, 169(7): 863 – 870

Falcon-Lang HJ, Kvaček J and Uličny D. 2001. Fire-prone plant communities and palaeoclimate of a Late Cretaceous fluvial to estuarine environment, Pecínov quarry, Czech Republic. Geological Magazine, 138(5): 563 – 576

Falcon-Lang HJ, Wheeler E, Baas P and Herendeen PS. 2012. A diverse charcoalified assemblage of Cretaceous (Santonian) angiosperm woods from Upatoi Creek, Georgia, USA. Part 1: Wood types with scalariform perforation plates. Review of Palaeobotany and Palynology, 184: 49 – 73

Finkelstein DB, Pratt LM, Curtin TM and Brassell SC. 2005. Wildfires and seasonal aridity recorded in Late Cretaceous strata from south-eastern Arizona, USA. Sedimentology, 52(3): 587 – 599

Fiorillo AR, Adams TL and Kobayashi Y. 2012. New sedimentological, palaeobotanical, and dinosaur ichnological data on the palaeoecology of an unnamed Late Cretaceous rock unit in Wrangell-St. Elias National Park and Preserve, Alaska, USA. Cretaceous Research, 37: 291 – 299

Francis JE and Coffin MF. 1992. Cretaceous fossil wood from the Raggatt Basin, southern Kerguelen Plateau (site 750). Proceedings of the Ocean Drilling Program, Scientific Results, 120: 273 – 280

Friedman WE. 2009. The meaning of Darwin's 'abominable mystery'. American Journal of Botany, 96(1): 5 – 21

Friis EM, Pedersen KR and Crane PR. 2006. Cretaceous angiosperm flowers: Innovation and evolution in plant reproduction. Palaeogeography, Palaeoclimatology, Palaeoecology, 232(2 – 4): 251 – 293

Friis EM, Crane PR and Pedersen KR. 2019. Extinct diversity among Early Cretaceous angiosperms: Mesofossil evidence of early Magnoliales from Portugal. International Journal of Plant Sciences, 180(2): 93 – 127

Fung MK, Schaller MF, Hoff CM, Katz ME and Wright JD. 2019. Widespread and intense wildfires at the Paleocene-Eocene boundary. Geochemical Perspectives Letters, 10: 1 – 6

Gajendiran K, Kandasamy S and Narayanan M. 2024. Influences of wildfire on the forest ecosystem and climate change: A comprehensive study. Environmental Research, 240: 117537

Gaskell DE, Huber M, O'Brien CL, Inglis GN, Acosta RP, Poulsen CJ and Hulla PM. 2022. The latitudinal temperature gradient and its climate dependence as inferred from foraminiferal $\delta^{18}O$ over the past 95 million years. Proceedings of the National Academy of Sciences of the United States of America, 119(11): e2111332119

Glasspool IJ and Scott AC. 2010. Phanerozoic concentrations of atmospheric oxygen reconstructed from sedimentary charcoal. Nature Geoscience, 3(9): 627 – 630

Goldberg ED. 1985. Black Carbon in the Environment: Properties and Distribution. New York: John Wiley, 1 – 199

Greguš J, Kvaček J and Sakala J. 2020. Charcoalified homoxylous woods from the Cenomanian of the Bohemian Cretaceous Basin (Czech Republic). Review of Palaeobotany and Palynology, 282: 104311

Grice K, Nabbefeld B and Maslen E. 2007. Source and significance of selected polycyclic aromatic hydrocarbons in sediments (Hovea-3 well, Perth Basin, Western Australia) spanning the Permian-Triassic boundary. Organic Geochemistry, 38(11): 1795 – 1803

Guatame C and Rincón M. 2021. Coal petrology analysis and implications in depositional environments from upper Cretaceous to Miocene: A study case in the Eastern Cordillera of Colombia. International Journal of Coal Science & Technology, 8(5): 869 – 896

Haq BU. 2014. Cretaceous eustasy revisited. Global and Planetary Change, 113: 44 – 58

Harrison SP, Marlon JR and Bartlein PJ. 2010. Fire in the earth system. In: Dodson J (ed.). Changing Climates, Earth Systems and Society. Dordrecht: Springer, 21 – 48

Hasegawa T. 2001. Predominance of terrigenous organic matter in Cretaceous marine fore-arc sediments, Japan and Far East Russia. International Journal of Coal Geology, 47(3 – 4): 207 – 221

Hasegawa T and Hibino T. 2011. Polycyclic aromatic hydrocarbons in the Jurassic-Cretaceous Tetori Group, central Japan. Island Arc, 20(1): 23 – 34

He TH, Pausas JG, Belcher CM, Schwilk DW and Lamont BB. 2012. Fire-adapted traits of *Pinus* arose in the fiery Cretaceous. New Phytologist, 194(3): 751 – 759

Hedges JI, Eglinton G, Hatcher PG, Kirchman DL, Arnostie C, Derenne S, Evershed RP, Kögel-Knabner I, de Leeuw JW, Littkej R, Michaelis W and Rullkötter J. 2000. The molecularly-uncharacterized component of nonliving organic matter in natural environments. Organic Geochemistry, 31(10): 945 – 958

Heimhofer U, Hochuli PA, Burla S, Dinis JML and Weissert H. 2005. Timing of Early Cretaceous angiosperm diversification and possible links to major paleoenvironmental change. Geology, 33(2): 141 – 144

Herendeen PS. 1991. Charcoalified angiosperm wood from the Cretaceous of eastern North America and Europe. Review of Palaeobotany and Palynology, 70(3): 225 – 239

Herendeen PS and Skog JE. 1998. Gleichenia chaloneri: A new fossil fern from the Lower Cretaceous (Albian) of England. International Journal of Plant Sciences, 159(5): 870 – 879

Hu XM, Li J, Han Z and Li YX. 2020. Two types of hyperthermal events in the Mesozoic-Cenozoic: Environmental impacts, biotic effects, and driving mechanisms. Science China (Earth Sciences), 63(8): 1041 – 1058

Huber BT, MacLeod KG, Watkins DK and Coffin MF. 2018. The rise and fall of the Cretaceous Hot Greenhouse climate. Global and Planetary Change, 167: 1 – 23

Huber M and Caballero R. 2003. Eocene El Niño: Evidence for robust tropical dynamics in the "Hothouse". Science, 299(5608): 877 – 881

Huber M and Caballero R. 2011. The Early Eocene equable climate problem revisited. Climate of the Past, 7(2): 603 – 633

Hyland EG and Sheldon ND. 2013. Coupled CO_2-climate response during the Early Eocene Climatic Optimum. Palaeogeography, Palaeoclimatology, Palaeoecology, 369: 125 – 135

Inglis GN, Bragg F, Burls NJ, Cramwinckel MJ, Evans D, Foster GL, Huber M, Lunt DJ, Siler N, Steinig S, Tierney JE, Wilkinson R, Anagnostou E, de Boer AM, Jones TD, Edgar KM, Hollis CJ, Hutchinson DK and Pancost RD. 2020. Global mean surface temperature and climate sensitivity of the Early Eocene Climatic Optimum (EECO), Paleocene-Eocene Thermal Maximum (PETM), and latest Paleocene. Climate of the Past, 16(5): 1953 – 1968

International Committee for Coal and Organic Petrology (ICCP). 2001. The new inertinite classification (ICCP System 1994). Fuel, 80(4): 459 – 471

Jiang HH and Lee CTA. 2019. On the role of chemical weathering of continental arcs in long-term climate regulation: A case study of the Peninsular Ranges batholith, California (USA). Earth and Planetary Science Letters, 525: 115733

Jones MW, Smith A, Betts R, Canadell JG, Prentice IC and Le Quéré C. 2020. Climate change increases the risk of wildfires. https://www.jstor.org/stable/resrep51248

Jones TP, Scott AC and Cope M. 1991. Reflectance measurements and the temperature of formation of modern charcoals and implications for studies of fusain. Bulletin de la Société Géologique de France, 162(2): 193 – 200

Jones TP, Scott AC and Mattey DP. 1993. Investigations of "fusain transition fossils" from the Lower Carboniferous: Comparisons with modern partially charred wood. International Journal of Coal Geology, 22(1): 37 – 59

Judd EJ, Tierney JE, Lunt DJ, Montañez IP, Huber BT, Wing SL and Valdes PJ. 2024. A 485-million-year history of Earth's surface

temperature. Science, 385(6715): eadk3705
Karp AT, Holman AI, Hopper P, Grice K and Freeman KH. 2020. Fire distinguishers: Refined interpretations of polycyclic aromatic hydrocarbons for paleo-applications. Geochimica et Cosmochimica Acta, 289: 93 – 113
Kiehl JT, Zarzycki CM, Shields CA and Rothstein MV. 2021. Simulated changes to tropical cyclones across the Paleocene-Eocene Thermal Maximum (PETM) boundary. Palaeogeography, Palaeoclimatology, Palaeoecology, 572: 110421
Klages JP, Salzmann U, Bickert T, Hillenbrand CD, Gohl K, Kuhn G, Bohaty SM, Titschack J, Müller J, Frederichs T, Bauersachs T, Ehrmann W, van de Flierdt T, Pereira PS, Larter RD, Lohmann G, Niezgodzki I, Uenzelmann-Neben G, Zundel M, Spiegel C, Mark C, Chew D, Francis JE, Nehrke G, Schwarz F, Smith JA, Freudenthal T, Esper O, Pälike H, Ronge TA, Dziadek R and the Science Team of Expedition PS104. 2020. Temperate rainforests near the South Pole during peak Cretaceous warmth. Nature, 580 (7801): 81 – 86
Knight TK, Bingham PS, Grimaldi DA, Anderson K, Lewis RD and Savrda CE. 2010. A new Upper Cretaceous (Santonian) amber deposit from the Eutaw Formation of eastern Alabama, USA. Cretaceous Research, 31(1): 85 – 93
Kostova I, Zdravkov A, Bechtel A, Botoucharov N, Groβ D, Dochev D and Apostolova D. 2022. Characterization of organic matter from the Cretaceous sedimentary and volcano-sedimentary strata from Livingston Island, Antarctic Peninsula: Insights from organic petrology, molecular proxies and carbon and hydrogen isotopes. International Journal of Coal Geology, 252: 103940
Kraal P, Slomp CP, Forster A and Kuypers MMM. 2010. Phosphorus cycling from the margin to abyssal depths in the proto-Atlantic during oceanic anoxic event 2. Palaeogeography, Palaeoclimatology, Palaeoecology, 295(1 – 2): 42 – 54
Kuhlbusch TAJ. 1998. Black carbon and the carbon cycle. Science, 280 (5371): 1903 – 1904
Kumar M. 2018. Evidence of wildfire based on microscopic charcoal, spores and pollen grains from Early Cretaceous sediments of South Rewa and Kachchh basins, India. Journal of Palaeosciences, 67(1 – 2): 147 – 169
Kumar R, Hameed A and Srivastava P. 2023. Clay mineralogical evidence of near-equatorial Palaeocene-Eocene Thermal Maximum in Barmer Basin, India. Clay Minerals, 58(2): 121 – 142
Kvaček J and Eklund H. 2003. A report on newly recovered reproductive structures from the Cenomanian of Bohemia (Central Europe). International Journal of Plant Sciences, 164(6): 1021 – 1039
Lamberson MN, Bustin RM, Kalkreuth WD and Pratt KC. 1996. The formation of inertinite-rich peats in the mid-Cretaceous Gates Formation: Implications for the interpretation of mid-Albian history of paleowildfire. Palaeogeography, Palaeoclimatology, Palaeoecology, 120(3 – 4): 235 – 260
Lee CTA and Lackey JS. 2015. Global continental arc flare-ups and their relation to long-term Greenhouse conditions. Elements, 11(2): 125 – 130
Lei Y, Cao HR, Wang XY, Zhang DP, Wang WB and Guo XL. 2022. Polycyclic aromatic hydrocarbons in the Upper Cretaceous lacustrine deposits from the Songliao Basin (NE China): Implications for wildfires and paleoclimate. Palaeogeography, Palaeoclimatology, Palaeoecology, 600: 111083
Lenz OK, Riegel W and Wilde V. 2021. Greenhouse conditions in Lower Eocene coastal wetlands? Lessons from Schöningen, Northern Germany. PLoS One, 16(1): e0232861
Li MS, Kump LR, Ridgwell A, Tierney JE, Hakim GJ, Malevich SB, Poulsen CJ, Tardif R, Zhang HX and Zhu J. 2024. Coupled decline in ocean pH and carbonate saturation during the Palaeocene-Eocene Thermal Maximum. Nature Geoscience, 17(12): 1299 – 1305
Li YY, Hou SF and Zhao PF. 2010. Comparison of different quantification methods for microfossil charcoal concentration and the implication for human activities. Quaternary Sciences, 30(2): 356 – 363 (in Chinese with English abstract)
Lidgard S and Crane PR. 1988. Quantitative analyses of the early angiosperm radiation. Nature, 331(6154): 344 – 346
Lidgard S and Crane PR. 1990. Angiosperm diversification and Cretaceous floristic trends: A comparison of palynofloras and leaf macrofloras. Paleobiology, 16(1): 77 – 93
Lima ALC, Farrington JW and Reddy CM. 2005. Combustion-derived polycyclic aromatic hydrocarbons in the environment: A review. Environmental Forensics, 6(2): 109 – 131
Lü DW, Du WX, Zhang ZH, Gao Y, Wang TT, Xu JC, Zhang AC and Wang CS. 2024. A synthesis of the Cretaceous wildfire record related to atmospheric oxygen levels? Journal of Palaeogeography, 13 (1): 149 – 164
Lu M, Ikejiri T and Lu YH. 2021. A synthesis of the Devonian wildfire record: Implications for paleogeography, fossil flora, and paleoclimate. Palaeogeography, Palaeoclimatology, Palaeoecology, 571: 110321
Lupia R, Lidgard S and Crane PR. 1999. Comparing palynological abundance and diversity: Implications for biotic replacement during the Cretaceous angiosperm radiation. Paleobiology, 25(3): 305 – 340
Manfroi J, Dutra TL, Gnaedinger S, Uhl D and Jasper A. 2015. The first report of a Campanian palaeo-wildfire in the West Antarctic Peninsula. Palaeogeography, Palaeoclimatology, Palaeoecology, 418: 12 – 18
Manfroi J, Trevisan C, Dutra TL, Jasper A, Carvalho MDA, Aquino FE and Leppe M. 2023. "Antarctic on fire": Paleo-wildfire events associated with volcanic deposits in the Antarctic Peninsula during the Late Cretaceous. Frontiers in Earth Science, 11: 1048754
Martill DM, Loveridge RF, Mohr BAR and Simmonds E. 2012. A wildfire origin for terrestrial organic debris in the Cretaceous Santana Formation Fossil Lagerstätte (Araripe Basin) of north-east Brazil. Cretaceous Research, 34: 135 – 141
Masiello CA. 2004. New directions in black carbon organic geochemistry. Marine Chemistry, 92(1 – 4): 201 – 213
Mays C, Cantrill DJ and Bevitt JJ. 2017. Polar wildfires and conifer serotiny during the Cretaceous global hothouse. Geology, 45(12): 1119 – 1122
Mays C and Cantrill DJ. 2019. Protodammara reimatamoriori, a new species of conifer (Cupressaceae) from the Upper Cretaceous Tupuangi Formation, Chatham Islands, Zealandia. Alcheringa: An Australasian Journal of Palaeontology, 43(1): 114 – 126
McLauchlan KK, Higuera PE, Miesel J, Rogers BM, Schweitzer J, Shuman JK, Tepley AJ, Varner JM, Veblen TT, Adalsteinsson SA, Balch JK, Baker P, Batllori E, Bigio E, Brando P, Cattau M, Chipman ML, Coen J, Crandall R, Daniels L, Enright N, Gross WS, Harvey BJ, Hatten JA, Hermann S, Hewitt RE, Kobziar LN, Landesmann JB, Loranty MM, Maezumi SY, Mearns L, Moritz M, Myers JA, Pausas JG, Pellegrini AFA, Platt WJ, Roozeboom J, Safford H, Santos F, Scheller RM, Sherriff RL, Smith KG, Smith MD and Watts AC. 2020. Fire as a fundamental ecological process: Research advances and frontiers. Journal of Ecology, 108(5): 2047 – 2069
Miller KG, Browning JV, Schmelz WJ, Kopp RE, Mountain GS and Wright JD. 2020. Cenozoic sea-level and cryospheric evolution from deep-sea geochemical and continental margin records. Science Advances, 6(20): eaaz1346
Mills BJW, Krause AJ, Jarvis I and Cramer BD. 2023. Evolution of atmospheric O_2 through the Phanerozoic, revisited. Annual Review of Earth and Planetary Sciences, 51: 253 – 276
Moore EA and Kurtz AC. 2008. Black carbon in Paleocene-Eocene boundary sediments: A test of biomass combustion as the PETM trigger. Palaeogeography, Palaeoclimatology, Palaeoecology, 267(1 – 2): 147 – 152
Moore TA, Moroeng OM, Shen J, Esterle JS and Pausch RC. 2021. Using carbon isotopes and organic composition to decipher climate and tectonics in the Early Cretaceous: An example from the Hailar Basin, Inner Mongolia, China. Cretaceous Research, 118: 104674
Nakamura H, Sawada K and Takahashi M. 2010. Aliphatic and aromatic

terpenoid biomarkers in Cretaceous and Paleogene angiosperm fossils from Japan. Organic Geochemistry, 41(9): 975 – 980

Nichols GJ, Cripps JA, Collinson ME and Scott AC. 2000. Experiments in waterlogging and sedimentology of charcoal: Results and implications. Palaeogeography, Palaeoclimatology, Palaeoecology, 164(1 – 4): 43 – 56

Nunes F and Norris RD. 2006. Abrupt reversal in ocean overturning during the Palaeocene/Eocene warm period. Nature, 439(7072): 60 – 63

Page SE, Siegert F, Rieley JO, Boehm HDV, Jaya A and Limin S. 2002. The amount of carbon released from peat and forest fires in Indonesia during 1997. Nature, 420(6911): 61 – 65

Pang Y, Zhou B, Zhou X, Xu XC, Liu XY, Zhan T and Lu YH. 2021. Abundance and $\delta^{13}C$ of sedimentary black carbon indicate rising wildfire and C4 plants in Northeast China during the Early Holocene. Palaeogeography, Palaeoclimatology, Palaeoecology, 562: 110075

Peng Y, Jiang RX, Shi C, Song WC, Long XX, Engel MS and Wang S. 2022. Alitrepaninae, a new subfamily of auger beetles from mid-Cretaceous Kachin amber of northern Myanmar (Coleoptera: Bostrichidae). Cretaceous Research, 137: 105244

Penman DE, Hönisch B, Zeebe RE, Thomas E and Zachos JC. 2014. Rapid and sustained surface ocean acidification during the Paleocene-Eocene Thermal Maximum. Paleoceanography, 29(5): 357 – 369

Pole MS and Douglas JG. 1999. Bennettitales, cycadales and ginkgoales from the mid-Cretaceous of the Eromanga Basin, Queensland, Australia. Cretaceous Research, 20(5): 523 – 538

Price C and Rind D. 1994. The impact of a $2 \times CO_2$ climate on lightning-caused fires. Journal of Climate, 7(10): 1484 – 1494

Pross J, Contreras L, Bijl PK, Greenwood DR, Bohaty SM, Schouten S, Bendle JA, Röhl U, Tauxe L, Raine JI, Huck CE, Van De Flierdt T, Jamieson SSR, Stickley CE, van de Schootbrugge B, Escutia C and Brinkhuis H. 2012. Persistent near-tropical warmth on the Antarctic continent during the Early Eocene epoch. Nature, 488(7409): 73 – 77

Rajak PK, Singh VK and Singh PK. 2019. Distribution of inertinites in the Early Paleogene lignites of Western India: On the possibility of wildfire activities. Journal of the Geological Society of India, 93(5): 523 – 532

Schlanger SO and Jenkyns HC. 1976. Cretaceous oceanic anoxic events: Causes and consequences. Geologie en Mijnbouw, 55(3): 179 – 184

Schnyder J, Dejax J, Keppens E, Tu TTN, Spagna P, Boulila S, Galbrun B, Riboulleau A, Tshibangu JP and Yans J. 2009. An Early Cretaceous lacustrine record: Organic matter and organic carbon isotopes at Bernissart (Mons Basin, Belgium). Palaeogeography, Palaeoclimatology, Palaeoecology, 281(1 – 2): 79 – 91

Scotese CR. 2016. PALEOMAP PaleoAtlas for GPlates and the PaleoData plotter program. PALEOMAP Project. https://www.earthbyte.org/paleomap-paleoatlas-for-gplates/

Scotese CR, Song HJ, Mills BJW and van deer Meer DG. 2021. Phanerozoic paleotemperatures: The earth's changing climate during the last 540 million years. Earth-Science Reviews, 215: 103503

Scotese CR, Vérard C, Burgener L, Elling RP and Kocsis AT. 2025. The Cretaceous world: Plate tectonics, palaeogeography and palaeoclimate. In: Hart MB, Batenburg SJ, Huber BT, Price GD, Thibault T, Wagreich M and Walaszczyk I (eds.). Cretaceous Project 200 Volume 1: The Cretaceous World. Geological Society, London, Special Publications, 544(1): 31 – 202

Scott AC. 1989. Observations on the nature and origin of fusain. International Journal of Coal Geology, 12(1 – 4): 443 – 475

Scott AC. 2000. The Pre-Quaternary history of fire. Palaeogeography, Palaeoclimatology, Palaeoecology, 164(1 – 4): 281 – 329

Scott AC and Glasspool IJ. 2006. The diversification of Paleozoic fire systems and fluctuations in atmospheric oxygen concentration. Proceedings of the National Academy of Sciences of the United States of America, 103(29): 10861 – 10865

Scott AC. 2010. Charcoal recognition, taphonomy and uses in palaeoenvironmental analysis. Palaeogeography, Palaeoclimatology, Palaeoecology, 291(1 – 2): 11 – 39

Scott AC. 2019. The use of charcoal to interpret Cretaceous wildfires and volcanic activity. Global Geology, 22(4): 217 – 241

Shao LY, Zhou JM, Jones TP, Hua FH, Xu XT, Yan ZM, Hou HH, Wang DD and Lu J. 2024. Inertinite in coal and its geoenvironmental significance: Insights from AI and big data analysis. Science China (Earth Sciences), 67(6): 1779 – 1801

Shukla A, Jasper A, Uhl D, Mathews RP, Singh VP, Chandra K, Chetia R, Shukla S and Mehrotra RC. 2023. Paleo-wildfire signatures revealing co-occurrence of angiosperm-gymnosperm in the Early Paleogene: Evidences from woody charcoal and biomarker analysis from the Gurha lignite mine, Rajasthan, India. International Journal of Coal Geology, 265: 104164

Smith DM, Griffin JJ and Goldberg ED. 1973. Elemental carbon in marine sediments: A baseline for burning. Nature, 241(5387): 268 – 270

Smith DM and Chughtai AR. 1995. The surface structure and reactivity of black carbon. Colloids and Surfaces A: Physicochemical and Engineering Aspects, 105(1): 47 – 77

Smith T, Rose KD and Gingerich PD. 2006. Rapid Asia-Europe-North America geographic dispersal of earliest Eocene primate *Teilhardina* during the Paleocene-Eocene Thermal Maximum. Proceedings of the National Academy of Sciences of the United States of America, 103(30): 11223 – 11227

Suman DO, Kuhlbusch TAJ and Lim B. 1997. Marine sediments: A reservoir for black carbon and their use as spatial and temporal records of combustion. In: Clark JS, Cachier H, Goldammer JG and Stocks B (eds.). Sediment Records of Biomass Burning and Global Change. Berlin Heidelberg: Springer, 271 – 293

Sweeney IJ, Chin K, Hower JC, Budd DA and Wolfe DG. 2009. Fossil wood from the middle Cretaceous Moreno Hill Formation: Unique expressions of wood mineralization and implications for the processes of wood preservation. International Journal of Coal Geology, 79(1 – 2): 1 – 17

Synnott DP, Schwark L, Dewing K, Pedersen PK and Sanei H. 2021. Evidence for widespread wildfires and their environmental impact in the Late Cretaceous Canadian Arctic. Global and Planetary Change, 203: 103515

Taylor DW and Hickey LJ. 1996. Evidence for and implications of an herbaceous origin for angiosperms. In: Taylor DW and Hickey LJ (eds.). Flowering Plant Origin, Evolution & Phylogeny. Boston: Springer, 232 – 266

The Cenozoic CO_2 Proxy Integration Project (CenCO_2PIP) Consortium. 2023. Toward a Cenozoic history of atmospheric CO_2. Science, 382(6675): eadi5177

Thomas E. 2007. Cenozoic mass extinctions in the deep sea: What perturbs the largest habitat on earth? In: Monechi S, Coccioni R and Rampino M (eds.). Large Ecosystem Perturbations: Causes and Consequences. Boulder: Geological Society of America, 1 – 23

Tierney JE, Zhu J, Li MS, Ridgwell A, Hakim GJ, Poulsen CJ, Whiteford RDM, Rae JWB and Kump LR. 2022. Spatial patterns of climate change across the Paleocene-Eocene Thermal Maximum. Proceedings of the National Academy of Sciences of the United States of America, 119(42): e2205326119

Tosolini AMP, Korasidis VA, Wagstaff BE, Cantrill DJ, Gallagher SJ and Norvick MS. 2018. Palaeoenvironments and palaeocommunities from Lower Cretaceous high-latitude sites, Otway Basin, southeastern Australia. Palaeogeography, Palaeoclimatology, Palaeoecology, 496: 62 – 84

Turgeon SC and Creaser RA. 2008. Cretaceous oceanic anoxic event 2 triggered by a massive magmatic episode. Nature, 454(7202): 323 – 326

Uhl D, Jasper A, Solórzano Kraemer MM and Wilde V. 2019. Charred biota from an Early Cretaceous fissure fill in W-Germany and their palaeoenvironmental implications. Neues Jahrbuch für Geologie und Paläontologie-Abhandlungen, 293(1): 83 – 105

Vajda V, Fernández MDP, Villanueva-Amadoz U, Lehsten V and Alcalá

L. 2016. Dietary and environmental implications of Early Cretaceous predatory dinosaur coprolites from Teruel, Spain. Palaeogeography, Palaeoclimatology, Palaeoecology, 464: 134 – 142

Valdes PJ, Scotese CR and Lunt DJ. 2021. Deep ocean temperatures through time. Climate of the Past, 17(4): 1483 – 1506

van der Werf GR, Randerson JT, Giglio L, van Leeuwen TT, Chen Y, Rogers BM, Mu MQ, van Marle MJE, Morton DC, Collatz GJ, Yokelson RJ and Kasibhatla PS. 2017. Global fire emissions estimates during 1997 – 2016. Earth System Science Data, 9(2): 697 – 720

van Dijk J, Fernandez A, Bernasconi SM, Caves Rugenstein JK, Passey SR and White T. 2020. Spatial pattern of super-greenhouse warmth controlled by elevated specific humidity. Nature Geoscience, 13(11): 739 – 744

Viehofen A, Hartkopf-Fröder C and Friis EM. 2008. Inflorescences and flowers of Mauldinia *angustiloba* sp. nov. (Lauraceae) from Middle Cretaceous karst infillings in the Rhenish Massif, Germany. International Journal of Plant Sciences, 169(7): 871 – 889

von Strandmann PAEP, Jenkyns HC and Woodfine RG. 2013. Lithium isotope evidence for enhanced weathering during Oceanic Anoxic Event 2. Nature Geoscience, 6(8): 668 – 672

Walters AP, Tierney JE, Zhu J, Meyers SR, Graves K and Carroll AR. 2023. Climate system asymmetries drive eccentricity pacing of hydroclimate during the Early Eocene greenhouse. Science Advances, 9(31): eadg8022

Walters GL, Kemp SJ, Hemingway JD, Johnston DT and Hodell DA. 2022. Clay hydroxyl isotopes show an enhanced hydrologic cycle during the Paleocene-Eocene Thermal Maximum. Nature Communications, 13(1): 7885

Wang J, Zhou XY and Li XQ. 2024. A study of wildfire evolution during the Paleocene-Eocene warm period in the northern hemisphere. Quaternary Sciences, 44(1): 1 – 15 (in Chinese with English abstract)

Wang S, Shao LY, Yan ZM, Shi MJ and Zhang YH. 2019. Characteristics of Early Cretaceous wildfires in peat-forming environment, NE China. Journal of Palaeogeography, 8(1): 17

Wang X. 2004. Plant cytoplasm preserved by lightning. Tissue and Cell, 36(5): 351 – 360

Wang XT, Chen ZL, Cui LL and Wang X. 2025. Spatiotemporal evolution of wildfire activity during the Paleocene-Eocene Thermal Maximum in China. Science China (Earth Sciences), 68(2): 509 – 522

Wang ZW, Xu Y, Zhao QJ, Zhang MM, Li WX, Panchal B and Liu BJ. 2023. Peatland wildfires in the Lower Cretaceous Damoguaihe Formation, Hailar Basin, Northeast China. Cretaceous Research, 150: 105578

Westerhold T, Marwan N, Drury AJ, Liebrand D, Agnini C, Anagnostou C, Barnet JSK, Bohaty SM, De Vleeschouwer D, Florindo F, Frederichs T, Hodell DA, Holbourn AE, Kroon D, Lauretano V, Littler K, Lourens LJ, Lyle M, Pälike H, Röhl U, Tian J, Wilkens RH, Wilson PA and Zachos JC. 2020. An astronomically dated record of Earth's climate and its predictability over the last 66 million years. Science, 369(6509): 1383 – 1387

Willard DA, Donders TH, Reichgelt T, Greenwood DR, Sangiorgi F, Peterse F, Nierop KGJ, Frieling J, Schouten S and Sluijs A. 2019. Arctic vegetation, temperature, and hydrology during Early Eocene transient global warming events. Global and Planetary Change, 178: 139 – 152

World Meteorological Organization (WMO). 2025. State of the global climate 2024. https://wmo.int/publication-series/state-of-global-climate-2024

Xu XT, Shao LY, Eriksson KA, Zhou JM, Wang DD, Hou HH, Hilton J, Wang S, Lu J and Jones TP. 2022. Widespread wildfires linked to early Albian Ocean Anoxic Event 1b: Evidence from the Fuxin lacustrine basin, NE China. Global and Planetary Change, 215: 103858

Yans J, Spagna P, Gerards T, Gerrienne P, Dejax J, Gomez B, Dupuis C, Baele JM, Barbier F and Pirson S. 2009. The Lower Cretaceous Wealden facies of the Hautrage quarry (Mons Basin, Belgium). In: Proceedings of the Darwin-Bernissart Meeting. Brussels, 137 – 145

Zachos JC, McCarren H, Murphy B, Röhl U and Westerhold T. 2010. Tempo and scale of Late Paleocene and Early Eocene carbon isotope cycles: Implications for the origin of hyperthermals. Earth and Planetary Science Letters, 299(1 – 2): 242 – 249

Zhang MZ, Dai S, Du BX, Ji LM and Hu SS. 2018. Mid-Cretaceous Hothouse climate and the expansion of early angiosperms. Acta Geologica Sinica, 92(5): 2004 – 2025

Zhang SH, Ji WQ and Chen HB. 2022. Advances of driving mechanisms of the Early Eocene Climatic Optimum (EECO): Constraints from the Linzizong volcanic rocks in southern Tibet. Acta Petrologica Sinica, 38(5): 1313 – 1327 (in Chinese with English abstract)

Zhang ZH, Lü DW, Wang TT, An DZ, Liu HY, Wang DD and Wang CS. 2022. Intensive peatland wildfires during the Aptian-Albian oceanic anoxic event 1b: Evidence from borehole SK-2 in the Songliao Basin, NE China. Journal of Palaeogeography, 11: 448 – 467

Zhou XY, Wang J, Li Q, Bai B, Mao FY, Li XQ and Wang YQ. 2023. Late Paleocene to Early Oligocene fire ecology of the south Mongolian highland. Frontiers in Earth Science, 11: 1171452

Zhu MB, Song JZ, Tong XN, Hu JF, Xi DP, Cao HR, Peng PA and Wan XQ. 2017. The records of black carbon from Songliao Basin, Northeast China in Late Santonian, and their paleoenvironment implication. Earth Science Frontiers, 24(1): 166 – 173 (in Chinese with English abstract)

Zhu MB. 2019. Quantitative separation of black carbon in Cretaceous geological samples and its stable carbon isotope study. Ph. D. Dissertation. Beijing: University of Chinese Academy of Sciences, 99 – 115 (in Chinese with English abstract)

附中文参考文献

陈祚伶. 2022. 古新世-始新世极热事件碳循环研究进展. 科学通报, 67(15): 1704 – 1714

胡修棉, 李娟, 韩中, 李永祥. 2020. 中新生代两类极热事件的环境变化、生态效应与驱动机制. 中国科学(地球科学), 50(8): 1023 – 1043

李宜垠, 侯树芳, 赵鹏飞. 2010. 微炭屑的几种统计方法比较及其对人类活动的指示意义. 第四纪研究, 30(2): 356 – 363

邵龙义, 周家民, Jones TP, 华芳辉, 徐小涛, 闫志明, 侯海海, 王东东, 鲁静. 2024. 煤中惰质组及其古环境意义:来自 AI 和大数据分析的启示. 中国科学(地球科学), 54(6): 1806 – 1829

王建, 周新郢, 李小强. 2024. 古新世-始新世暖期北半球野火演化研究. 第四纪研究, 44(1): 1 – 15

王学婷, 陈祚伶, 崔琳琳, 王旭. 2025. 中国大陆古新世-始新世极热事件时期野火的时空演变. 中国科学(地球科学), 55(2): 524 – 536

张少华, 纪伟强, 陈厚彬. 2022. 早始新世气候适宜期的驱动机制研究进展: 来自藏南林子宗火山岩的制约. 岩石学报, 38(5): 1313 – 1327

祝孟博, 宋建中, 童晓宁, 胡建芳, 席党鹏, 曹怀仁, 彭平安, 万晓樵. 2017. 松辽盆地晚三冬期的黑碳记录及其古环境意义. 地学前缘, 24(1): 166 – 173

祝孟博. 2019. 白垩纪地质样品中黑碳的定量分离及其稳定碳同位素研究. 博士学位论文. 北京: 中国科学院大学, 99 – 115